

Aerodynamic design optimization: Challenges and perspectives

Joaquim R.R.A. Martins¹

Department of Aerospace Engineering, University of Michigan, Ann Arbor, MI, 48109, USA

ARTICLE INFO

Keywords:

Aerodynamic design optimization
Aerodynamic shape optimization
Computational fluid dynamics
Aerostructural optimization
Airfoil optimization
Wing design

ABSTRACT

Antony Jameson pioneered CFD-based aerodynamic design optimization in the late 1980s. In addition to developing the fundamental theory, Jameson implemented that theory in codes that were practical enough to be used in industry. As a result of Jameson's seminal efforts, a research community has been established in aerodynamic design optimization. This research area has experienced sustained improvements in CFD solvers, mesh deformation, sensitivity computation, and optimization tools. We review recent developments for each of these components and present open-source tools available for aerodynamic shape optimization. A variety of applications is presented, including the optimization of a supercritical airfoil starting from a circle, a web application that optimizes airfoils within a few seconds, aircraft aerodynamic and aerostructural optimization, and aeropropulsive optimization. We also review the Aerodynamic Design Optimization Discussion Group (ADODG) benchmarks and other aerodynamic shape optimization problems. Among the ADODG benchmarks, we focus on the RANS-based problems and discuss some of the issues encountered, including comparing Euler and RANS results and design-space multimodality. The availability of these benchmarks and the open-source tools is expected to enable further studies and benchmarks in CFD-based aerodynamic design optimization and MDO.

1. Introduction

The development of computational fluid dynamics (CFD) and advances in parallel computing hardware revolutionized the aerodynamic design process. CFD is now routinely used in industry, and it is hard to imagine a design process without using it. While CFD has improved the design process, there is a potential to improve it even further by integrating it with numerical optimization to perform design optimization.

When CFD was first introduced in industry, it was met with skepticism by seasoned aerodynamicists, who were, in part, concerned with having their role diminished by this new tool. Eventually, it became clear that CFD was just that: a new tool that aerodynamicists could leverage to analyze and understand the design. This required aerodynamicists to learn the new tool and to adjust their role in the analysis and design process.

Because the end goal is not just to understand the design but also to find out how to make the design better, CFD analysis is not enough. Coupling CFD analysis with numerical optimization emerged as a way to improve designs more effectively. However, CFD-based aerodynamic design optimization faces a predicament similar to CFD when it was first introduced to industry decades ago. This new tool is set to change the aerodynamic design process, but it faces several challenges. Although the new generation of aerodynamicists tends

to have a strong CFD background, a stronger background in design optimization is increasingly important.

In this paper, we focus on significant challenges that must be addressed to broaden the use of aerodynamic design optimization in industry, and how these challenges are being addressed. These challenges include: (1) CFD solver robustness, (2) scalability with the number of design variables, (3) efficient and accurate gradient computation, (4) geometry parametrization, (5) robust mesh deformation, (6) availability of specialized software, (7) practical industrial constraints, including consideration of aircraft design disciplines other than aerodynamics. This paper reviews the efforts to address these challenges.

Some of these challenges were cited in the CFD Vision 2030 study [1]. One of the “grand challenges” outlined in that study is the multidisciplinary analysis and optimization of a highly flexible advanced aircraft configuration, which relates to Challenge 7, but requires all the other challenges we list to be addressed as well. Many of the developments described in the present paper contribute directly to milestones listed in the CFD Vision 2030 study.

Key challenges that are not discussed here include optimization under uncertainty and mesh generation and adaptation. Uncertainty quantification for CFD models with arbitrary probability distributions is by itself a costly proposition [2]. Performing optimization under

E-mail address: jrram@umich.edu.

¹ This is a review paper summarizing already published results. Please see the references for the original contributors.

uncertainty compounds this already high cost to the point where it is currently not a feasible proposition. However, robust designs assuming normal distributions can be obtained with multipoint optimizations [3]. Mesh generation is an issue that we address here partially. While we address automatic mesh deformation within the optimization cycle, fully automated generation of the initial mesh is still a holy grail in CFD. Automatic mesh adaptation has tremendous potential for aerodynamic shape optimization, especially when the mesh is adapted based on the objective and constraint functions [4–6].

The Aerodynamic Design Optimization Discussion Group (ADODG) benchmarks played a crucial role in the latest developments. Developing optimization problems that everyone could run and compare has motivated researchers to do an especially thorough job of getting the best possible optimized shapes and addressing computational bottlenecks. It also motivated us to make all the results publicly available and generate benchmarks within and beyond the scope of the ADODG. Finally, solving and discussing the ADODG benchmarks helped us understand our results and their limitations, motivating further developments.

The remainder of this paper is structured as follows. We explain the significance of Antony Jameson's groundbreaking contributions in Section 2, together with the developments in aerodynamic design optimization that have ensued. In Section 3, we present an overview of the developments that address the challenges listed above. In Section 4, we summarize the ADODG benchmarks and cite the efforts towards solving them. In Section 5, we highlight applications that we developed and investigated beyond the ADODG benchmarks. We end with concluding remarks in Section 6.

2. Jameson's contributions

The single most important development in aerodynamic shape optimization was the adjoint method, which computes derivatives of performance metrics of interest with respect to design variables efficiently and accurately. Together with gradient-based optimization, the adjoint method made it possible to optimize shapes parameterized using many variables. This was a crucial development because wing shape requires hundreds of design variables to utilize design optimization fully.

The adjoint method was first developed to solve optimal control problems, where it was used to optimize rockets and aircraft trajectories that were soon after that validated in flight tests [7]. An adjoint method was also developed to compute derivatives of finite-element models for structural optimization [8]. Pironneau [9] extended the adjoint method to achieve minimum drag shapes for Stokes flow and the incompressible Euler equations [10].

Antony Jameson then made a sequence of significant breakthroughs that made adjoint-based aerodynamic design optimization practical enough for industrial use [11]. He derived the adjoint for the compressible Euler equations and applied it to airfoil design [12] and wing design [13]. In this early work, “control theory” was often cited, where the shape in aerodynamic optimization replaced the trajectory in optimal control [14].

Hicks and Henne [15] had already integrated CFD with numerical optimization and demonstrated the potential for aerodynamic design optimization, developing what became known as Hicks–Henne functions to apply shape perturbations to parametrize the airfoil. However, they were limited to 11 design variables because they used finite differences to compute the required derivatives. On the other hand, Jameson [16] optimized shapes by changing the positions of thousands of surface mesh points, thanks to the efficiency of the adjoint method. He avoided issues with high-frequency shape oscillations by using a gradient-smoothing technique. Reuther and Jameson [17] implemented B-splines and Hick–Henne functions in their adjoint-based framework and compared the resulting shapes.

Reuther et al. [18] extended the applicability of adjoint optimization to large-scale problems with full-configuration, multiblock CFD meshes through improvements to the design parametrization method, mesh perturbation scheme, and parallel implementation. This culminated in the optimization of full configurations considering multiple flight conditions [19,20]. The development of the RANS adjoint [21–23] enabled the realization of more practical designs, especially in the transonic regime. Jameson et al. [24] details the approach and sequence of developments.

Jameson adopted the continuous approach to the adjoint derivations, which he inherited from the calculus of variations approach in optimal control. Using this approach, the partial differential equations of the governing equations are differentiated by hand before discretization. Jameson demonstrated mathematical prowess in his derivations of the continuous adjoint equations and ingenuity in applying the boundary conditions. He also devised the appropriate discretization schemes for the adjoint equations. Finally, he took the development process all the way to the software implementation and its application to aircraft design. His Fortran FLO and SYN codes are widely known and used by various aircraft manufacturers, including Airbus, Boeing, Bombardier, and Embraer.

Since Antony Jameson spearheaded these efforts, aerodynamic design optimization has benefited from many developments, in parallel with improvements in the CFD algorithms and computing hardware [11]. We review some of these developments in the remainder of this paper.

3. Challenges and developments

Despite several decades of developments in aerodynamic shape optimization, several challenges remain in its practical application and more widespread use. This section focuses on a few challenges that we have tackled in the last decade. This list of challenges is not meant to be comprehensive, but it addresses most of the challenges from the CFD Vision 2030 report [1].

3.1. CFD solver robustness

Integrating CFD in a numerical optimization cycle demands additional requirements on the robustness of the CFD solver. One of the reasons for this is that a CFD solver is more likely to fail during optimization because the optimizer does not have the designer's intuition. Therefore the optimization algorithm tends to provide bad design shapes to the CFD solver during the optimization. Therefore, the CFD solver must be able to solve for designs that might not make much sense. Another reason why robustness is essential is that in multidisciplinary analysis, the CFD solver is coupled to other disciplines that might provide unusual boundary conditions for the flow [1].

If the CFD solver fails to converge during an optimization iteration, it interrupts the optimization process, which must then be restarted. Some optimizers allow the user-provided functions to return a “fail” flag, which the optimizer accounts for by taking a less ambitious step for the subsequent function evaluation. While this might prevent the optimization from exiting outright, the optimization might still fail because the information from failed function evaluations is not as rich as a regular evaluation. Inaccurate information is still better than a “fail”, as long as it is sufficiently accurate to provide the correct trends—having the right sign in each gradient component is usually sufficient to guide the optimizer away from a bad design. Therefore, it is usually worthwhile to force the CFD solver to converge to a solution, even if that solution does not represent the actual physics.

To this end, we developed a Jacobian-free approximate Newton-Krylov strategy for robustly solving the RANS equations for a wide range of geometries. Yildirim et al. [25] describes this strategy in detail, and we only include a summary here. Fig. 1 shows an overview of the method. The solver updates the state at each nonlinear iteration using

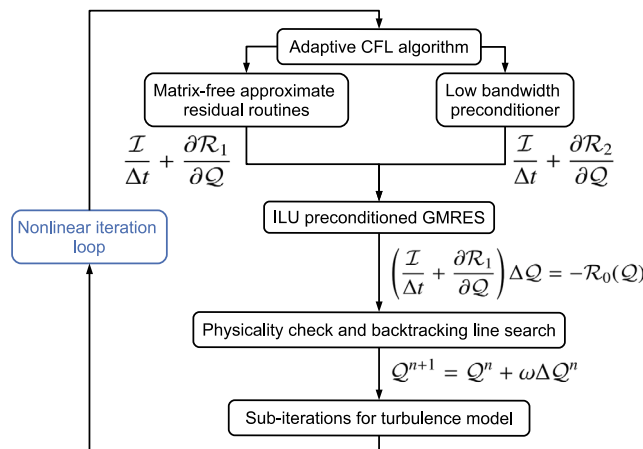


Fig. 1. Overview of the Jacobian-free approximate Newton–Krylov strategy.
Source: courtesy of Anil Yildirim.

the backward Euler time-stepping formula. To alleviate the problematic startup phase, it uses an adaptive CFL algorithm based on pseudo-transient continuation [26]. This starts with a small time step for robustness and then increases the step size rapidly as it approaches the solution. This exploits the favorable stability properties of the backward Euler method during the initial stage while approaching a Newton-type algorithm as the time step approaches infinity. At each nonlinear iteration, the update vector is obtained by inexactly solving a large linear system. We use two levels of approximation for the exact flow Jacobian residuals (R_0): R_1 and R_2 . R_1 is an approximation that leaves out several terms, but it is still closer to the exact Jacobian than R_2 (which is a first-order Jacobian approximation). R_1 is used for the GMRES matrix–vector products, and R_2 is used for the preconditioner. Since this is inexact, we make sure that the thermodynamic quantities do not vary by more than 20%, and we use a line search with backtracking to ensure a decrease in the unsteady residual norm.

At the same time, we lag the preconditioner for few nonlinear iterations. The use of approximate residual routines for the matrix-free driver improves the conditioning of the linear systems, which would be too costly to solve using exact routines.

We implemented the ANK approach in the ADflow open-source CFD solver [27].² ADflow can converge steady-state solutions to the RANS equations even if the flow field is inherently unsteady. This is owing to the backward Euler algorithm, which can stabilize the physically unstable modes. An example of such a flow solution is shown in Fig. 2, where NASA's Common Research Model (CRM) is solved for 90 deg angle of attack at $M = 0.85$. The solution, is not physical in this case, but the important thing is that the flow solver can converge. This case was inspired by the 90 deg angle-of-attack airfoil solution by Burgess and Glasby [28].

An example of such an optimization is the one performed by He et al. [29] using MACH-Aero, which starts from a circle and converges to a supercritical airfoil shape in a single fully automated optimization, as shown in Fig. 3. Again, the flow solution for the circle and some of the intermediate shapes are not physical, but the derivatives with respect to shape have the right trend for drag reduction. As the shape approaches the optimum, the RANS solution becomes valid. As long as the optimizer can eventually converge to a case where the solution is valid, inaccurate intermediate results are irrelevant.

3.2. Scaling with number of design variables

Aerodynamic shape optimization requires a large number of shape design variables to achieve the best possible performance. For transonic wing design optimization, Lyu et al. [30] showed that at least 200 shape variables are required to take full advantage of aerodynamic shape optimization. Beyond this number of variables, there are diminishing returns. Only gradient-based optimization algorithms can handle this number of variables efficiently. Fig. 4 shows the scalability of two gradient-free optimization algorithms (NSGA2 and ALPSO) compared to two gradient-based optimization algorithms (SLSQP and SNOPT) for a multidimensional Rosenbrock function. This figure demonstrates that gradient-based algorithms are the only viable option for more than 100 design variables. Furthermore, for a given gradient-based optimizer, there is a large difference between using finite differences (the default way gradient-based optimizers compute the gradients) and an analytic method (which in this case is based on the symbolic differentiation of the function and is thus fast). Therefore, there is a big motivation for developing methods for computing gradients efficiently. We discuss such methods in the next section.

To compare gradient-based and gradient-free optimization algorithms for a more practical problem, Lyu et al. [32] benchmarked various optimizers for a CFD-based wing twist optimization problem. The problem was limited to nine twist design variables and a rather coarse mesh so that the optimization with the gradient-free algorithms was achievable. The optimization problem was to minimize the drag coefficient subject to a lift coefficient constraint. Most gradient-based algorithms achieved optimality within 14 to 230 function evaluations, while the gradient-free algorithms required over 8000 evaluations. Pulliam et al. [33] found similar trends for an airfoil optimization problem.

For the vast majority of our work, we use SNOPT, a gradient-based algorithm that implements sequential quadratic programming and can handle nonlinear constraints [34]. To facilitate its use in our framework, we have wrapped SNOPT (a Fortran library) with Python through the pyOptSparse wrapper [35].³ In addition to facilitating the integration with the other modules of the framework, pyOptSparse provides a common interface to various optimization algorithms; to try a different algorithm, only a flag needs to be changed in the main run script. Using this feature, we were able to run all the results shown in Fig. 5 with minimal setup effort.

3.3. Effective computation of derivatives

As illustrated in Fig. 4, a good gradient-based algorithm is not sufficient; it is also necessary for the gradients to be computed accurately and efficiently. As mentioned earlier, the adjoint method pioneered by Jameson enables the accurate and efficient computation of gradients in high-dimensional spaces, which addresses this need. While adjoint methods are highly desirable for their efficiency, they also require a great implementation effort. Thus, by *effective* we mean that the approach for adjoint development provides a good balance between implementation effort, accuracy, and efficiency.

The early adjoint method developed by Jameson used the *continuous* approach [14]. Using this approach, he used calculus of variations on the partial differential equations (PDE) that govern the flow to obtain the adjoint equations and then discretized these equations to solve them for the desired derivatives.

In contrast, the *discrete* adjoint approach starts with the discretized governing equations. It differentiates those equations to obtain a linear system that is then solved to get the desired derivatives. When comparing the continuous and discrete approaches, Nadarajah and Jameson [36] concluded that the discrete approach was more costly than the

² <https://github.com/mdolab/adflow>

³ <https://github.com/mdolab/pyoptsparse>

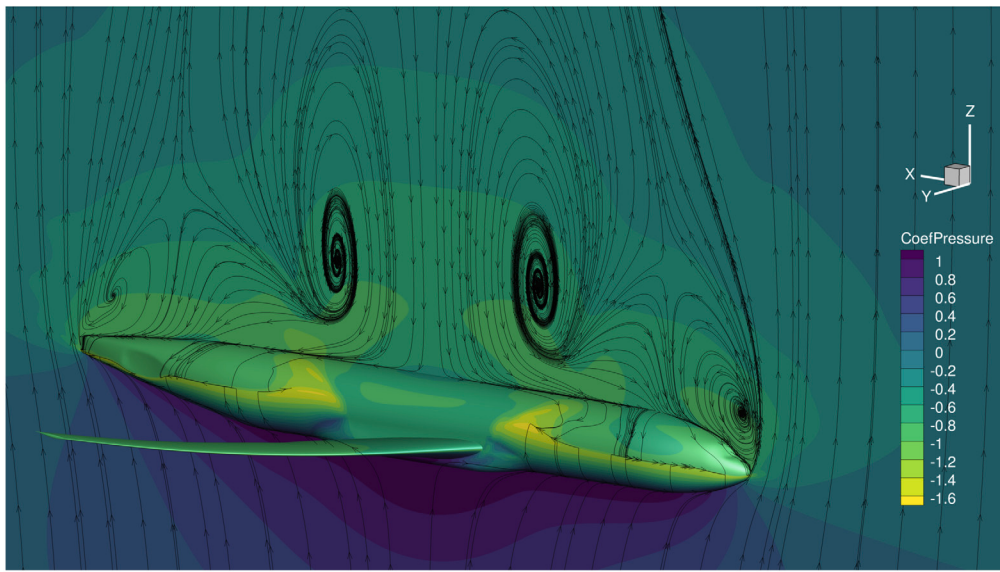


Fig. 2. Converged RANS solution for the CRM configuration at 90 deg angle of attack and $M = 0.85$ demonstrates the robustness of the ADflow solver.
Source: courtesy of Anil Yildirim.



Fig. 3. Lift- and moment-constrained drag minimization starting from a circle; $M = 0.734$, $C_l = 0.824$, $C_m \geq -0.092$ [29].

continuous approach and there was no benefit in the discrete approach. However, the discrete approach has been the preferred approach in the last decade because it is more straightforward to develop and because its gradients are consistent with the discretization [37–39].

To address the great implementation effort, we have developed a general recipe for effective adjoint method implementation that uses automatic differentiation (AD) to derive the terms needed for the discrete adjoint [40]. This approach had been previously mentioned by Giles and Pierce [37] and recommended in the survey by Peter and Dwight [39]. We have applied this approach to implement discrete adjoint methods to both ADflow [40] and OpenFOAM [41,42]. Similar approaches have been followed in the most recent adjoint implementations of the SU2 [43] and STAMPS flow solvers [44].

One unique feature of our approach is that we adopt a Jacobian-free GMRES strategy for the solution of the adjoint equations, which we found to be the most scalable [40]. The overall approach is illustrated in Fig. 6 using an extended design structure matrix (XDSM) representation [45].

3.4. Geometry parametrization

The early adjoint-based aerodynamic design efforts optimized shapes by directly changing the positions of all the CFD surface mesh

points. However, it is desirable to separate the geometry representation from the flow solver discretization to isolate the effects of mesh refinement from those of the geometry parametrization refinement and approach. This separation is also vital for modularity in computational framework settings, especially when performing multidisciplinary design optimization (MDO) [46].

To parametrize geometry for optimization, computer-aided design (CAD) is the natural choice given its universal use in industry. It allows designers to parametrize the geometry using variables that are intuitive to them. For seamless integration, designers should provide a CAD geometry as an input to the optimization process. Ideally, the optimization would use the parameters defined by the designers in CAD and output an optimized CAD geometry. This was also identified as a need in the CFD Vision 2030 report [1].

Past efforts that attempted to integrate CAD in aerodynamic shape optimization relied on finite differencing, which harmed the computational cost and accuracy of the derivatives [47,48]. Fortunately, recent efforts have focused on the computation of these derivatives [49–53].

Most researchers have implemented their own CAD-free geometry parametrization approaches, such as free-form deformation [54] and B-splines [55]. These parametrizations can be differentiated analytically and fully leverage the adjoint approach. There have been various studies comparing the different approaches, concluding that

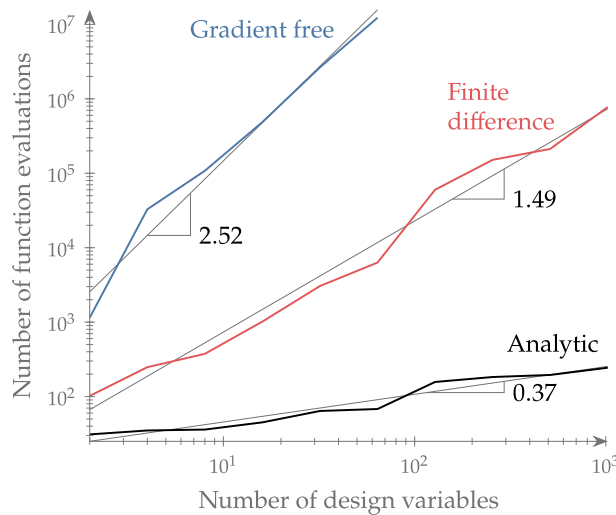


Fig. 4. Gradient-based optimization is the only hope for handling the large numbers of design variables required for aerodynamic shape optimization [31].

none of the geometry parametrization methods is superior to the others overall [56–60].

3.5. Mesh deformation

A shape optimization cycle requires a geometry engine to translate new shape design variables to new shapes and automatically obtain a new mesh for the new design surface. The new mesh is not regenerated, but rather, it is a deformation of the baseline mesh. The robustness of the mesh deformation is essential for the same reasons cited for flow solver robustness in Section 3.1: If it fails, it jeopardizes the optimization process. To address this need, we implemented IDWarp, an efficient analytic method for volume mesh deformation [61],⁴ which was also crucial in the airfoil optimization starting from a circle described in Section 3.1 [29].

The implementation is based on the inverse distance weighting proposed by Luke et al. [62], with some improvements. The most significant of these improvements is the efficient computation of derivatives via reverse-mode AD. More specifically, IDWarp computes the derivatives of all mesh point coordinates with respect to changes in the surface mesh point coordinates. This is one of the partial derivatives in the derivative chain between the aerodynamic force coefficients and the shape variables. Fig. 7 shows examples of mesh deformations performed with IDWarp for a wing mesh.

3.6. Software availability

One of the reasons why aerodynamic design optimization has not been more widely used is that it requires a complex set of tools that have not been readily available in the aerodynamic design community at large. Commercial CFD solvers have not implemented adjoint solvers until recently, and they have not been developed with optimization in mind. Other CFD-based optimization frameworks have been restricted to a few research groups in academia and government laboratories. One exception is the open-source CFD solver SU2, which includes an adjoint solver and provides aerodynamic shape optimization capability [63].

The capabilities described in the present paper are integrated into the MACH-Aero framework, which is available under an open-source

license.⁵ An XDSM of the aerodynamic shape optimization in MACH-Aero is shown in Fig. 8. All the components shown in the diagonal are wrapped in Python for modularity and ease of use. The optimizers are provided through the pyOptSparse interface introduced in Section 3.2. The geometry parametrization can use either our free-form deformation (FFD) implementation, pyGeo [54], or OpenVSP [64]. The volume mesh deformation is provided by IDWarp [61], which we introduced in Section 3.5. Either ADflow or OpenFOAM is available to solve the flow using a common Python interface. We envision that other CFD solvers could be easily integrated by wrapping them using the same Python interface, as described by Mader et al. [27]. Finally, as previously mentioned, both CFD solvers include an adjoint solver to compute the gradients for design optimization efficiently.

Even though gradient-based optimization with the adjoint method enables efficient aerodynamic shape optimization, it still requires hours on a parallel computer to converge an optimization fully. To make aerodynamic shape optimization more accessible, we have developed a web-based data-driven approach to airfoil design that takes just a few seconds for optimization [65].⁶ Fig. 9 shows a screenshot of this online tool, which includes a database of over 1500 airfoils.

3.7. Practical industrial design considerations

In addition to the challenges stated so far, there are several considerations needed for practical aerodynamic design. We start by discussing how to best integrate geometry in the industrial design process. We then present progress towards considering laminar-turbulent transition in aerodynamic design optimization, which is challenging in the three-dimensional case. We also discuss proposed approaches for constraining buffet, separation, cavitation, and flutter. Finally, we present progress towards including disciplines other than aerodynamics in the design optimization process, which is essential for practical design.

3.7.1. Geometry

Geometric constraints are also a necessity for practical aerodynamic shape optimization. Constraints such as variable fuel volume, wing thickness, leading-edge radius, and trailing edge angle constraints are linear and relatively easy to implement [30,54]. To consider geometric constraints implicitly, it is also possible to use a data-driven approach [66].

Spatial integration constraints are much more challenging. These are constraints that ensure that all the vehicle is to carry (people, payload, systems, and energy source) is contained within the outer mold line. Brelje et al. [67] developed a formulation for such constraints that includes efficient derivative computation. They demonstrated the feasibility of the approach by optimizing a shape enclosing a human avatar, as shown in Fig. 10. This approach was also demonstrated in the aerostructural design optimization of a wing with hydrogen fuel tanks, where the tanks were parameterized with CAD and allowed to change in size together with the wing shape and structural sizing [68].

As mentioned in Section 3.4, it would be desirable from the practical point of view to integrate CAD in the design optimization loop. For successful integration with an adjoint-based aerodynamic optimization framework, we require efficient computation of the derivatives of the CAD process, and this is the focus of current efforts [49,52,53]. Hopefully, CAD software vendors will support analytic derivatives in the near future.

⁴ <https://github.com/mdolab/idwarp>

⁵ <https://github.com/mdolab/MACH-Aero>

⁶ <http://webfoil.ingen.umich.edu>

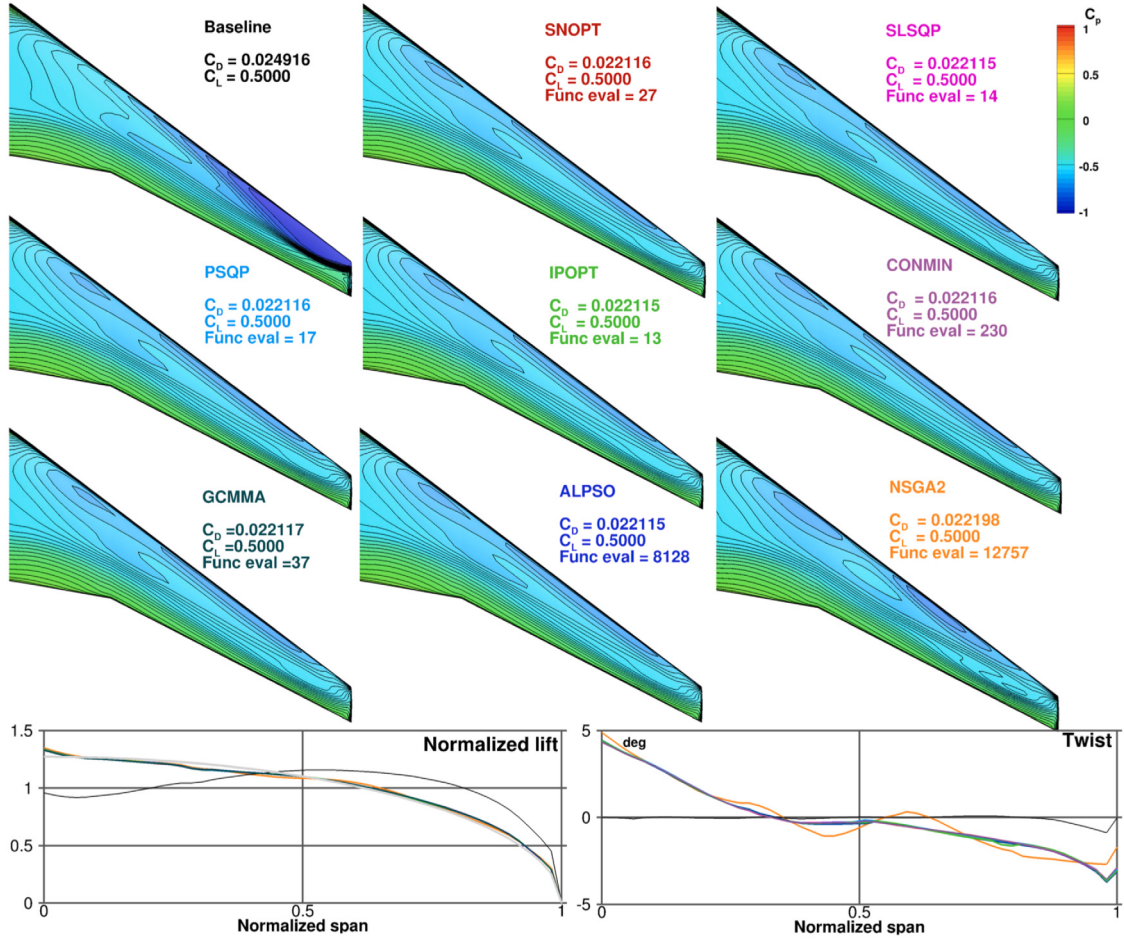


Fig. 5. Optimizer comparison for a wing design problem with nine twist variables shows that gradient-free methods cost 2–3 orders of magnitude more to optimize this simple problem [32].

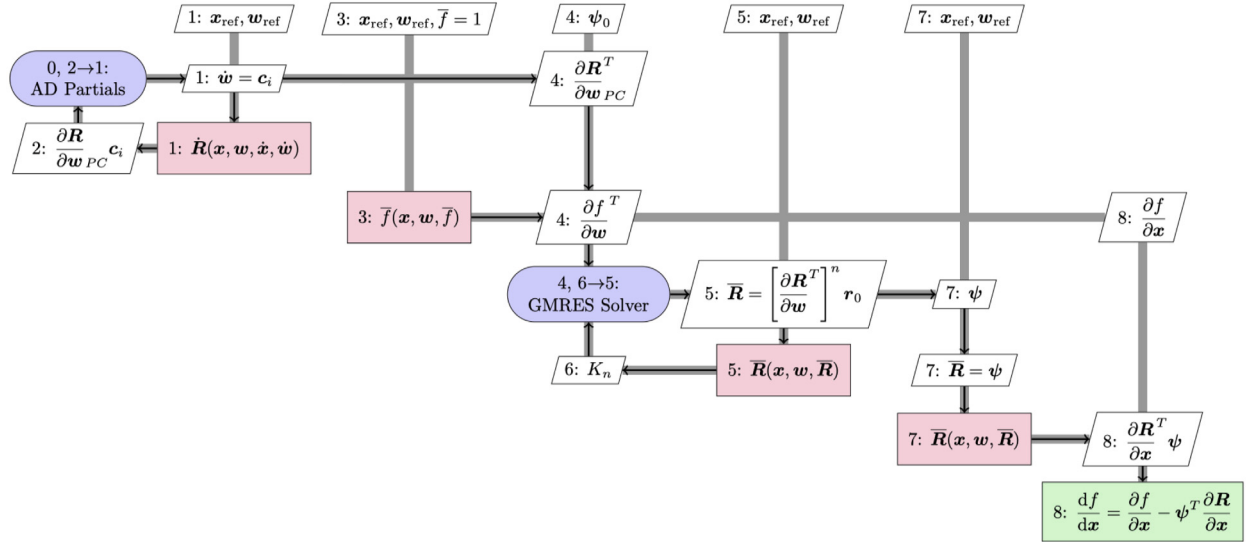


Fig. 6. XDSM of the hybrid-adjoint approach [40]. The transpose of the Jacobian ($(\partial R / \partial w)_{PC}^T$) is computed using forward mode AD and coloring in the 0, 2→1 loop. The adjoint equation right-hand side vector ($(\partial f / \partial w)^T$) is computed using reverse-mode AD in step 3. Then, the adjoint equation is solved using GMRES, and the resulting adjoint vector is used in step 8 to compute the desired total derivatives.

3.7.2. Laminar-turbulent transition

Most of the optimizations mentioned in this paper use RANS as a model and assume fully turbulent boundary layers. This assumption is acceptable for the high Reynolds numbers of transonic flight.

Although laminar flow is possible in this regime, the swept wings typical of transonic aircraft make it difficult to maintain a laminar boundary layer. Also, because laminar-turbulent transition is sensitive to surface imperfections and contamination, it is not safe to count

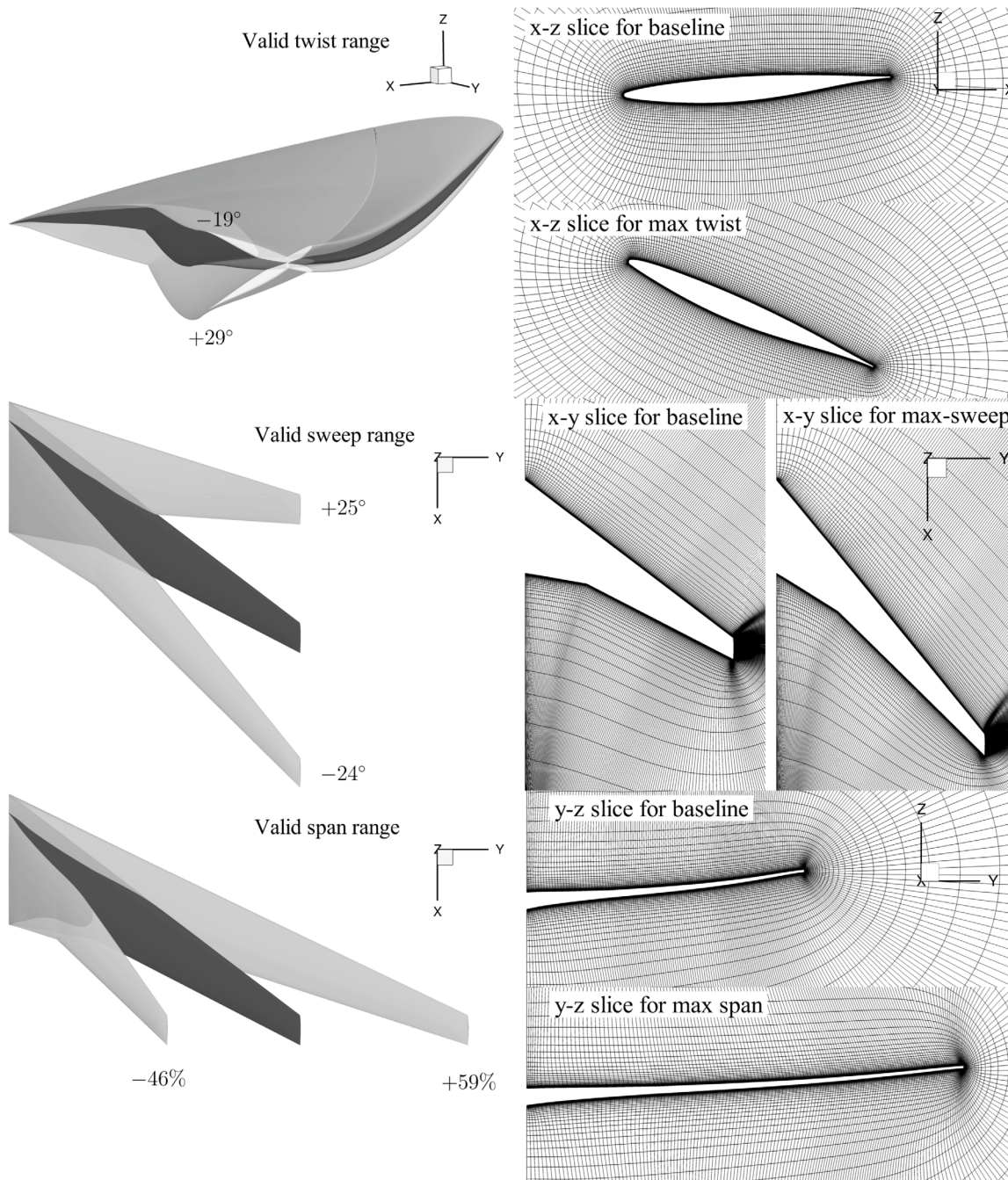


Fig. 7. Mesh deformations for wing planform optimization showing twist, sweep, and span variables [61].

on the lower drag in the aircraft range computations. Still, laminar-turbulent transition is essential for investigating future natural laminar flow (NLF) transonic aircraft. Considering laminar-turbulent transition is also essential in the design of lower Reynolds number aircraft with a significant amount of laminar flow, such as gliders, uninhabited aerial vehicles, and small transport aircraft.

When performing design optimization considering laminar-turbulent transition, we have two main choices of model: direct numerical simulation (DNS) and RANS [69]. In theory, DNS can predict the transition, including stages of linear development, nonlinear interactions, and turbulent spots. However, DNS is too expensive to use within an optimization loop [70].

Using RANS requires a way to predict the transition location. There are two main methods: the e^N method, which is based on stability

theory, and transition modeling methods [71]. The e^N method is usually coupled with linear stability theory (LST) and nonlinear parabolic stability equation (NPSE). LST can predict the linear development stage, while NPSE also considers nonlinear instabilities [72,73]. Unfortunately, NPSE is too computational costly for three-dimensional flows [74]. Since the linear stages can model most of the laminar-turbulent transition mechanisms, the e^N method based on LST has been used for designing aircraft, such as the Piaggio P180 [75], the Honda Jet [76], and the Boeing 757 ecoDemonstrator [77].

The transition modeling method was developed to be compatible with modern, unstructured parallelized CFD codes [78,79]. This method was extended to predict the significant crossflow-vortex induced transition [80,81]. Given the success of RANS-based aerodynamic shape optimization [30,40], the transition modeling method would be the ideal prediction method for considering transition in

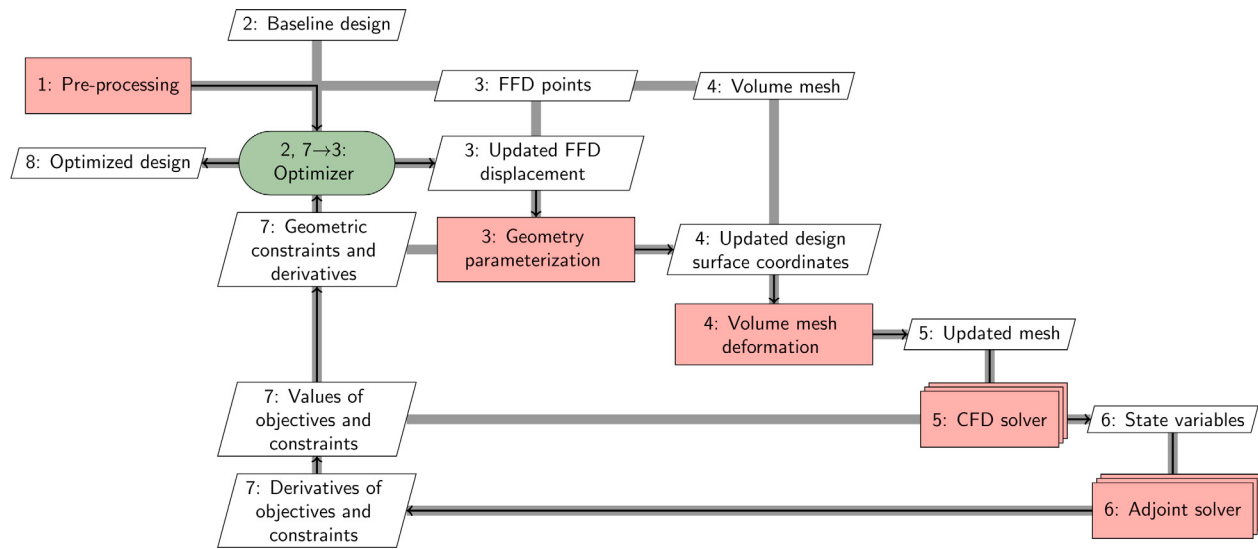


Fig. 8. XDSM of the open-source aerodynamic shape optimization framework, MACH-Aero.

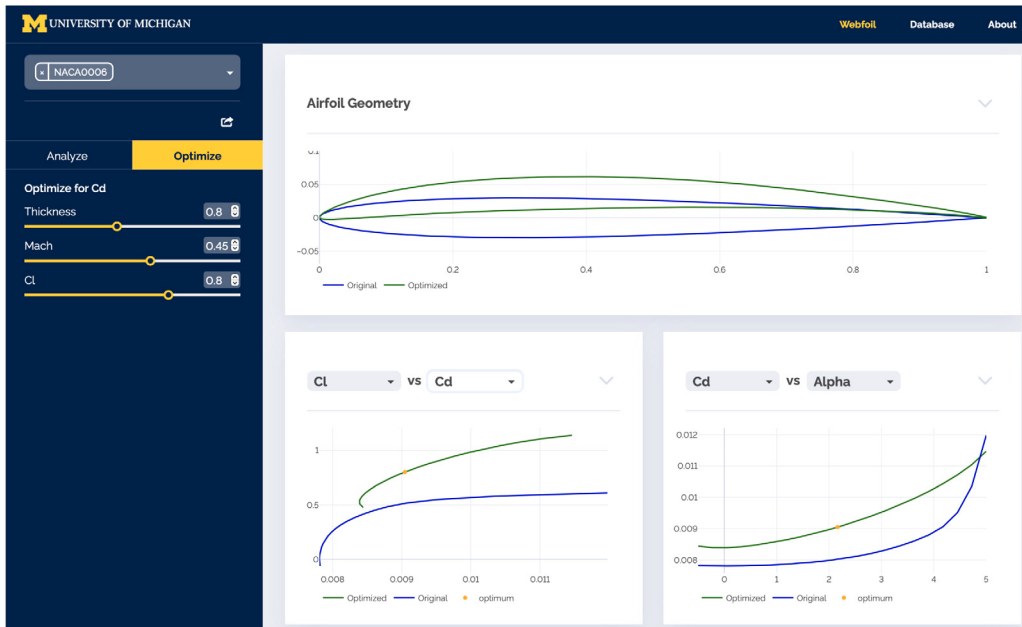


Fig. 9. Webfoil is an online database and airfoil optimization tool.

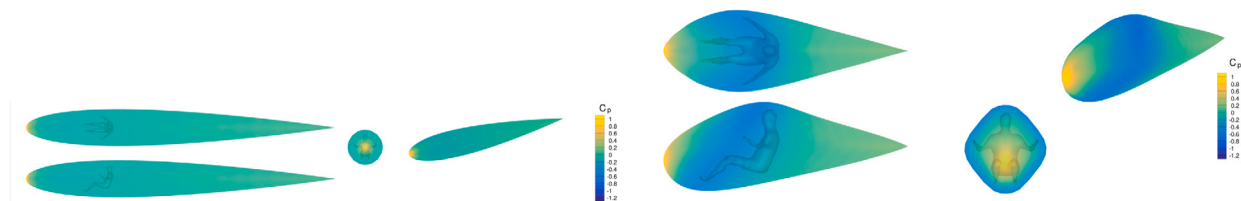


Fig. 10. Aerodynamic shape optimization of a surface enclosing a human avatar. The starting geometry is an axisymmetric surface of revolution with a NACA 0012 profile (left). The optimized shape (right) reduces the surface area and finds the optimal trade between skin friction and viscous pressure drag [67].

design optimization. Preliminary adjoint-based NLF optimization has been implemented by Khayatzadeh and Nadarajah [82] and by Halila et al. [83]. Unfortunately, the transition modeling method ignores

some of the transition mechanisms and involves parameter calibrations, which limit its practicality. This is mostly used for verification with benchmark cases, such as NLF-7301 airfoils [84], S809 airfoils [85], M6 wing [86], DLR F5 [78] wing and the 6:1 inclined prolate spheroid [80].

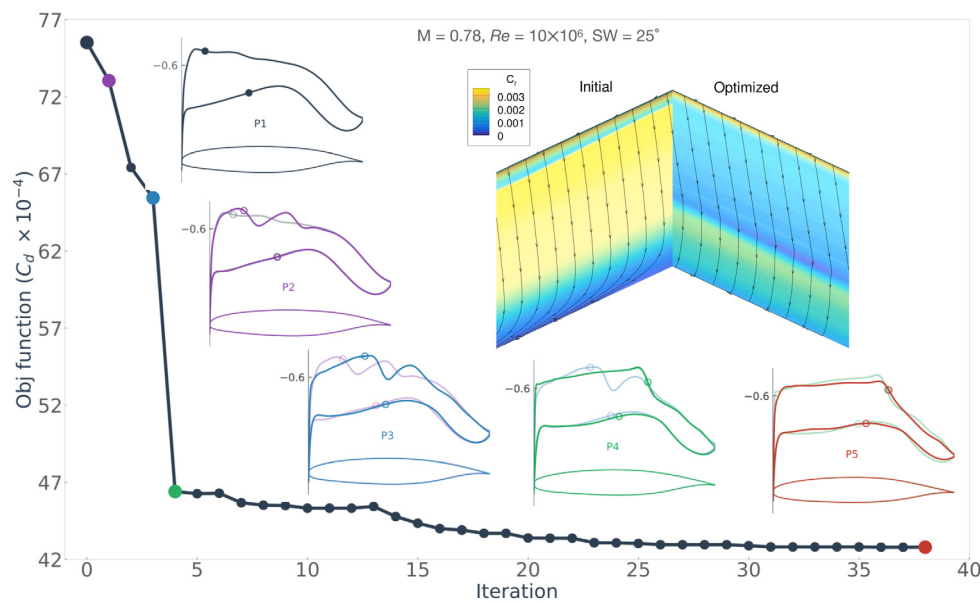


Fig. 11. Aerodynamic shape optimization considering laminar-turbulent transition, showing the initial and optimized C_f contour comparison on the upper surface, as well as the optimization convergence history [92].

Overall, the e^N method based on LST is the most promising NLF aerodynamic shape optimization approach because of the tractable computational cost. This method was used in RANS optimization frameworks for airfoil design using adjoint derivative computation [87–89]. The simplified e^N method proposed by Perraud et al. [90] was integrated with ADflow by Shi et al. [91] with a fully analytic coupled-adjoint implementation. The resulting NLF optimization framework predicts three-dimensional flow transition with Tollmien–Schlichting and crossflow instabilities. It is a promising tool for NLF wing design, as shown in Fig. 11 [92].

3.7.3. Buffet, separation, and cavitation

Constraints such as buffet and flutter are highly nonlinear and require much more development effort. Because these phenomena are time-dependent, it is challenging to simulate them in an optimization loop, and alternatives are needed to make the problem tractable.

Buffet is a phenomenon that is caused by shock-induced separation and is undesirable because it causes vibration. We developed a constraint formulation for buffet based on a separation sensor function [93], which was shown to be effective in various applications [94–99]. The approach is based on static simulations and avoids the prohibitive computational cost of running unsteady simulations in the optimization loop. Constraining buffet is crucial in transonic wing design. In Fig. 12 we compare the fuel burn contours for a single-point optimization without buffet constraints to a multipoint optimization with buffet constraints. The unconstrained single-point optimization achieves a high performance outside the buffet margin, and thus this high performance is not usable in practice. The buffet-constrained optimization moves the area of high performance and the 30% margin boundary so that the highest performance region is usable.

The separation sensor approach that Kenway and Martins [93] developed to constrain buffet depends on setting the appropriate value for the constraint on separated flow area. For the CRM, this value was determined by using two sources of information: The C_L curve given by CFD and experimental data [100]. In that case, the two sources agreed with each other, and the constraint value was shown to correlate well with buffet onset for the two Mach numbers of the experiment [93]. However, this value is not guaranteed to be valid for other aircraft and further investigation is needed. Buffet is a complex unsteady phenomenon that requires time-accurate well-resolved CFD [101]. While

researchers have been developing high-fidelity buffet models [102–105], using such models in a design optimization loop is currently prohibitive because of the high computational cost.

The separation sensor approach has also been used for low-speed performance. Bons and Martins [106] performed a wing aerostructural optimization where in addition to minimizing the fuel burn at the cruise condition ($M = 0.85$); they constrained the separation at a lower speed ($M = 0.4$) that did not contribute to the fuel burn computation. They found that the low-speed constraint resulted in much more realistic airfoils, as shown in Fig. 13. The airfoils optimized, including the low-speed separation constraint, have a larger leading edge radius than the other airfoils, which have sharp leading edges. Typically, thickness constraints are required to avoid sharp leading edges [30], but enforcing the low-speed separation constraint addresses the underlying issue using a constraint based on the physics.

To constrain cavitation in hydrofoil design optimization, we developed an approach that is mathematically identical to the buffet separation sensor constraint [107,108]. The difference is that instead of setting a constraint on the separation area, we set a constraint on the area that has a pressure below the vapor pressure.

3.7.4. Flutter

Flutter is yet another critical consideration that is especially relevant when the optimization includes wing planform variables. Jonsson et al. [109] reviewed the various approaches available for constraining flutter in aircraft design optimization, building on a previous review by Livne and Li [110]. For aircraft with more flexible, larger aspect ratio wings, nonlinear effects become more significant, and it becomes necessary to consider post-flutter limit cycle oscillation (LCO) [109, 111].

Similar to other optimization constraints, enforcing flutter or LCO constraints requires an acceptable computational cost, sufficient function smoothness, model robustness, and derivative computation. Several efforts succeeded in performing wing design optimization with respect to structural sizing [112,113]. However, aerodynamic shape optimization considering flutter remains a challenge because the aerodynamic characteristics need to be recomputed at every optimization iteration. The doublet-lattice method (DLM) has been successful in flutter prediction, and they can be used for both structural sizing and wing planform design variables [114]. However, DLM is only

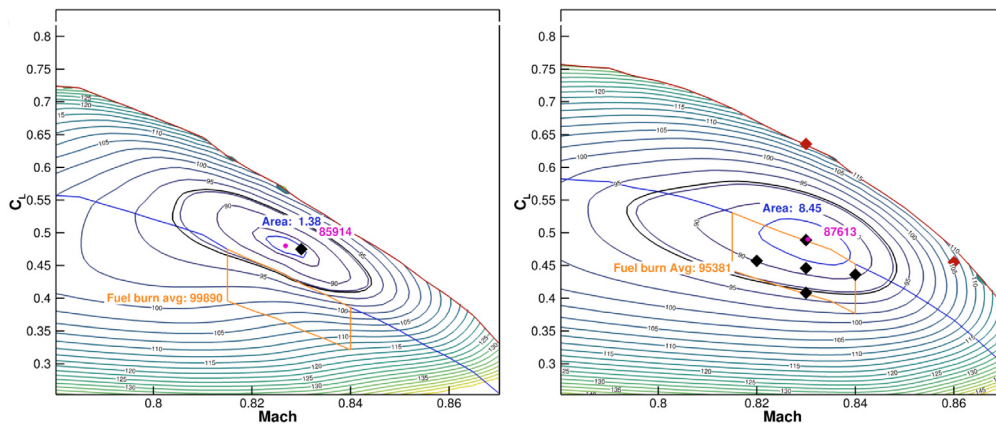


Fig. 12. Fuel burn contours and buffet boundary over the space of flight conditions (lift coefficient and Mach number) for a single-point optimization without buffet constraints (left) and multipoint optimization with buffet constraints (right). The red line represents the buffet boundary and the blue line represents the 30% margin to the boundary, which must not be exceeded in cruise flight conditions [93].

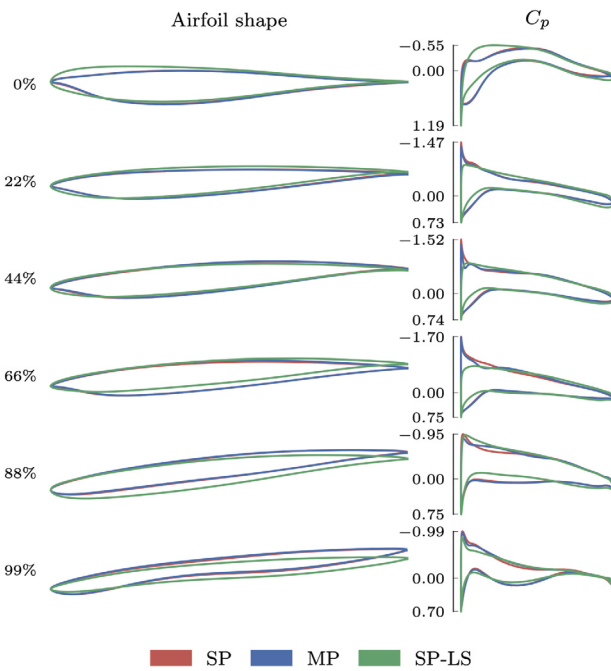


Fig. 13. Aerostructural wing optimization results for single point (SP), multipoint (MP), and single point with low-speed separation constraint (SP-LS), showing airfoils from the root (top) to the tip (bottom) [98].

suitable for subsonic flow conditions and does not consider airfoil shapes. CFD-based flutter computations are now possible, but including these computations in design optimization is still being developed. Time-domain methods remain prohibitive [115], but frequency-domain methods using time-spectral CFD show promise [116,117].

Like flutter, many other practical constraints require the consideration of disciplines beyond aerodynamics, which is the subject of the next section.

3.7.5. Multidisciplinary design optimization

Aerodynamics is not enough to achieve a feasible aircraft with high performance. The most critical other discipline is structures, which couples with aerodynamics to determine the wing performance. The coupling between the disciplines manifests itself both in analysis and design. The analysis requires solving a coupled system with both disciplines because the aerodynamic model provides the forces to the

structural model, while the structural model determines the displacements and hence the aerodynamic shape. From the design point of view, the optimal trade between structural weight and aerodynamic drag depends on the chosen objective function. Objective functions such as fuel burn and take-off weight depend on structural weight and drag, but in different proportions. Fuel burn places more emphasis on reducing drag, while take-off weight emphasizes reducing structural weight. More broadly, multidisciplinary design optimization (MDO) provides a way to model a coupled system and find optimal multidisciplinary design trades [118].

Given the motivation for efficient and accurate gradient computation, we developed a coupled-adjoint approach that computes gradients accounting for the aerostructural coupling [119]. To achieve this, we coupled ADflow to the open-source structural solver TACS, which has an adjoint solver [120]. The result was the MDO for aircraft configurations with high fidelity (MACH) framework. Using this approach, we can compute derivatives of aerodynamic forces and structural stresses with respect to structural sizing and aerodynamic shape variables.

MACH enabled us to perform the simultaneous design optimization of aerodynamic shape including wing planform variables and structural sizing for various aircraft design applications, including planform optimization starting from the CRM baseline [97], multimission fuel burn minimization [121], tow-steered composite optimization [99], and morphing wing optimization [122,123]. The MACH framework and these applications directly address the CFD 2030 Vision technology roadmap, which calls for a standard for coupling to other disciplines and CFD-based optimization of the entire aircraft [1].

The coupled-adjoint approach has also been generalized for an arbitrary number of disciplines [124], which lead to the modular analysis and unified derivatives (MAUD) architecture for MDO [125]. The MAUD architecture has been integrated into and improved upon in the OpenMDAO framework [126].

OpenMDAO has facilitated the coupling of CFD with other disciplines and the corresponding coupled adjoint derivative computations. Other MDO work beyond aerostructural optimization includes the simultaneous optimization of aerodynamic shape and propulsion system [127], and optimization of the wing, mission, and allocation [128, 129].

4. ADODG benchmarks

The ADODG benchmark development was motivated by the lack of comparisons between aerodynamic design optimization approaches and the lack of consensus on the characteristics of aerodynamic shape optimization problems. Each researcher had solved different problems using different approaches, making it difficult to compare the various

Table 1
ADODG benchmarks.

Case	Description	References
1	Drag minimization of the NACA 0012 in transonic inviscid flow.	[29,130–145]
2	Drag minimization of the RAE 2822 in transonic viscous flow	[29,130,131,133,136–140,143,146]
3	Lift-constrained drag minimization of a rectangular wing in inviscid subsonic flow	[131,133,136]
4	Lift-constrained drag minimization of the CRM wing in viscous flow	[30,32,131,133,136,144,147–149]
5	Lift-constrained drag minimization of the CRM wing–body–tail configuration at flight Reynolds number	[147,150]
6	Multimodal subsonic inviscid lift-constrained drag minimization	[151,152]

approaches. The ADODG developed a series of aerodynamic shape optimization problems of increasing complexity in geometry and physics. These benchmarks enable researchers to solve the same problem so that the results are more comparable.

Before the ADODG developed the benchmarks, the MDO Lab had been focusing on CFD-based wing aerostructural design optimization, which we introduced in Section 3.7.5. However, our early efforts solved the Euler equations for aerodynamics, and it was challenging to interpret the optimal design trends because they included both aerodynamic and structural effects. The ADODG benchmark cases (and Case 4 in particular), forced us to do more detailed studies considering aerodynamics alone. Understanding the aerodynamic shape optimization results then helped us understand the aerostructural results a lot better.

4.1. Summary of the ADODG benchmark cases

The ADODG benchmark problems are listed in Table 1, together with the references that tackled the respective problems. The objective for all problems is to minimize the drag coefficient (or a sum of drag coefficients in the multipoint cases). Most cases are subject to a lift coefficient constraint as well as thickness constraints. Some cases include a moment constraint as well.

The two first cases are airfoil shape optimization problems: Case 1 starts from a NACA 0012 airfoil baseline and Case 2 starts from the RAE 2822 airfoil. These two cases use different aerodynamic models: Case 1 solves the Euler equations, while Case 2 is based on the RANS equations. Another difference between these two cases is that Case 1 does not enforce a lift constraint, while Case 2 does. Based on the number of references, these two cases have been the most solved by far. This is in large part owing to the lower cost of solving two-dimensional cases.

Cases 3 and 4 optimize wing shapes; Case 3 is a subsonic case that solves the Euler equations, and Case 4 is a transonic case using RANS. Case 3 optimizes only twist, while Case 4 includes both twist and airfoil shapes. All wing cases include a volume constraint, where the volume of the optimized wing cannot decrease relative to the baseline wing.

Case 5 is an extension of Case 4 that adds the fuselage and tail. The baseline shape for Case 4 is the wing from the CRM full aircraft configuration clipped at the fuselage intersection. Case 5 restores the full CRM configuration and provides a benchmark for a more realistic

and industrially relevant design problem. It uses the flight Reynolds number (as opposed to the wind tunnel one), and the thickness constraints prevent the thickness from decreasing relative to the baseline CRM wing. It also includes a tail rotation angle design variable to trim the aircraft at various flight conditions. Case 5 adds two off-design flight conditions to prevent buffet [93].

Finally, Case 6 is a wing shape optimization problem similar to Case 3 with the addition of airfoil shape variables and planform variables (chord variation, sweep, span, and dihedral). The idea is to provide as much freedom in the design space exploration as possible and to determine the characteristics of the wing design problem in terms of multimodality.

4.2. Euler- versus RANS-based optimization

Although Cases 1 and 3 do not represent the actual physics, they challenge the numerical methods of the CFD, the parametrization approach, and the optimizer. Case 1, in particular, has received much attention even though the resulting shape is of no practical value. Such cases do have some value, and Case 1 has inspired and demonstrated new techniques. However, beyond a certain point, one might fall into the trap of developing solutions to issues that do not exist in practice. While RANS is more costly, many of the issues encountered with Euler-based shape optimization, such as non-unique solutions, disappear when using RANS. Also, we have found that for transonic wing shape optimization, Euler models resulted in entirely different shapes, as shown in Fig. 14 [153].

Another issue related to the impact of the model on the optimized shape is turbulence modeling. Overall, the choice of turbulence model does not affect the optimized shapes significantly. Vuruskan and Hosder [154] found that shape parametrization has a more significant impact than the choice of turbulence model, and Vuruskan and Hosder [155] found that the multipoint formulation was also more significant. When implementing the adjoint method, the turbulence model is sometimes not differentiated, resulting in gradients that do not account for the effect of the turbulence model. Lyu et al. [153] found that the effect of ignoring the turbulence model (called the “frozen turbulence” approach) resulted in a slightly inferior design and increased the computational cost of the optimization by 70%.

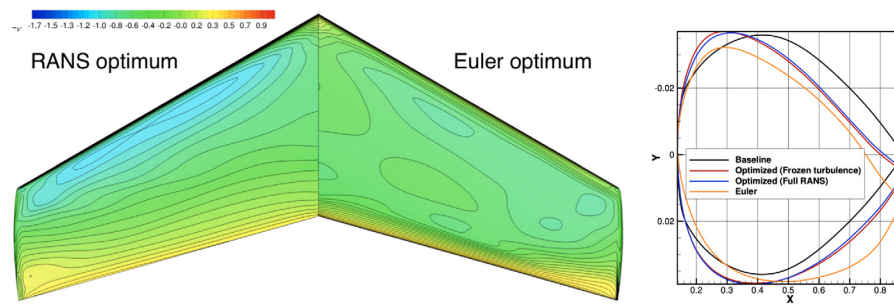


Fig. 14. Comparison between Euler- and RANS-based aerodynamic shape optimizations starting from the ONERA M6 wing. The RANS-optimized pressure distribution is better behaved and the optimal airfoils show large differences in shape [153].

4.3. RANS-based wing design optimization

As soon as the ADODG benchmark cases were established, we focused our first efforts on Case 4. This was because this was the most similar to the wing aerostructural design optimization that we had already been performing (see Section 3.7.5) [156].

Lyu et al. [30] reported our first results on Case 4.1, which was a single point optimization. The resulting wing, shown in Fig. 15, exhibits much thinner wing sections than the baseline CRM in the outboard sections, which also have sharper leading edges. This is because the case specifies that the airfoil thickness is allowed to be as low as 25% of the original CRM wing. The optimizer exploited this generous allowance to reduce the viscous pressure drag on the wing's outboard while thickening the inboard of the wing to satisfy the volume constraint. The thickening of the inboard increases the viscous pressure drag, but the decrease in the outboard more than compensates for this increase. Since the chord in the inboard is much larger, it is more efficient to increase the volume in this region to satisfy the volume constraint. Méheut et al. [147] verified this explanation by analyzing our optimal geometry with a drag decomposition tool. Not everyone achieved the same result. In some cases, the problem was not set up exactly as stated, but we suspect that in other cases, the gradients were not accurate enough. We found that the trade between outboard and inboard viscous pressure drag is subtle and requires many iterations with accurate gradients for the optimizer to find it.

Lyu et al. [30] also included the solution for a five-point multipoint problem before the ADODG added a series of multipoint problems to Case 4. The optimized shape for the multipoint case has less sharp leading edges. While the multipoint optimum does not exhibit a shock-free solution like its single-point counterpart, it represents an optimal compromise between the different flight conditions with a much more robust solution over the flight condition space.

Various multipoint cases (Cases 4.2–4.7) ranging from three to nine points were then added to the Case 4 ADODG benchmark. Kenway and Martins [157] solved and discussed all these cases, including a post-optimality study of the performance of the optimal wings over a range of flight conditions (defined by the lift coefficient and Mach number). The corresponding contour plots are shown in Fig. 16, where the contours were obtained by evaluating ML/D in a grid of RANS solutions for each optimal wing. In these plots, we can see that the larger the number of points considered, the more robust the design is to variations in the flight conditions. This robustness is achieved with a minor penalty in the maximum performance. One particularly interesting result is that of Case 4.5, which results in two maximum performance points with a region of lower performance between them.

4.4. Multimodality in aerodynamic shape optimization

A popular belief in the research community is that aerodynamic shape optimization problems are often multimodal. However, our studies have found that this concern is largely unwarranted. It is impossible

to prove that we have found the global optimum, but we only need to find a second local minimum to show that the problem is multimodal. As we describe in this section, we have shown convergence to unique optimal consistency for most of the ADODG cases, adding evidence to the hypothesis that these problems are unimodal and that we have found the global optimum.

In our first study of Case 4, we tried to find multiple local minima by starting from random perturbations of the original shape [30]. All optimizations converged to essentially the same shape. While we saw some difference in the shape design variables, the drag difference between the various designs was only 0.1 drag counts. Follow-up work by Yu et al. [149] found that refining the computational mesh brought these optimized shapes even closer to each other. That work included a starting design that consisted of a CRM planform with NACA 0012 airfoils and no twist, which also converged to the same Case 4 optimum. He et al. [29] performed a similar multi-start study for Case 2 and found that the optimization always converged to the same optimum airfoil, as shown in Fig. 17. Therefore, we hypothesize that the design space for twist and airfoil shape optimization is unimodal from the physical perspective. Around the global optimum, however, numerical noise causes gradient-based optimizers to converge to slightly different designs.

We believe that researchers often identify spurious multiple local minima because of numerical issues with either the computed gradients or the optimization algorithm. In ADflow, the adjoint gradients have been verified against the complex-step method [158]. Such verification of the computed gradients against an equally accurate method is recommended. We also recommend that practitioners pay close attention to the optimality and feasibility tolerances, as well as convergence histories. When using gradient-free algorithms, claimed optima are even more suspect. Unlike the mathematical optimality criteria of gradient-based algorithms, the optimality criteria for most gradient-free algorithms are based on heuristics.

4.5. Full configuration aerodynamic optimization and MDO

Case 4 considers only the wing from the Common Research Model (CRM) configuration and compensates by the lack of horizontal tail by imposing a moment coefficient constraint. While this design freedom provided an excellent test for the overall optimization procedure by requiring robustness to changes in the shape and accurate gradients, the optimal wings were too thin to be practical.

Case 5, builds upon Case 4, by considering the full CRM configuration (wing, fuselage, and horizontal tail), also known as the Drag Prediction Workshop (DPW) 4 geometry [159]. By adding back the fuselage and horizontal tail, we can enforce trim by changing the horizontal tail rotation and capturing the wing shape's true effect on trim drag. Chen et al. [150] investigated this effect and created a surrogate model for the trim drag to use when the horizontal tail is not available in the CFD model.

As mentioned in Section 3.7.5, aerodynamics is not enough for aircraft design. Inspired by the success of the ADODG benchmarks, we

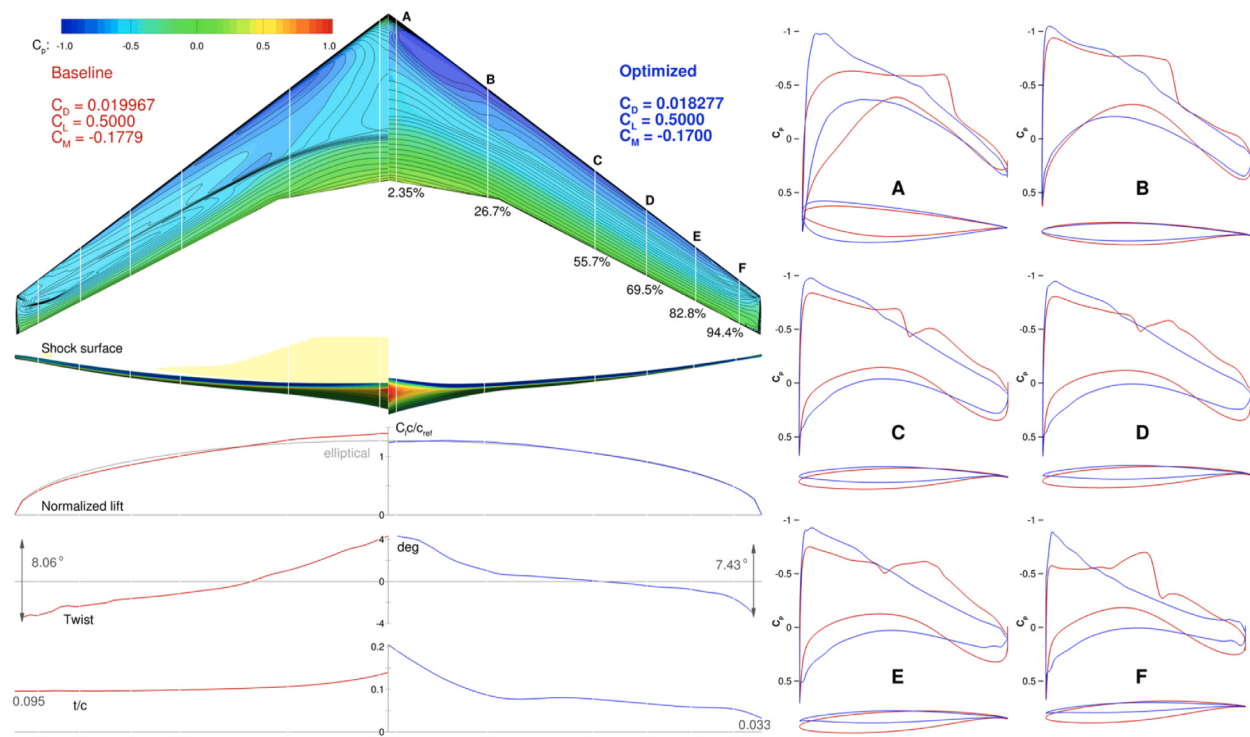


Fig. 15. Single-point optimization result for Case 4 [30].

developed an aerostructural wing design benchmark based on Case 5. This required creating a wingbox structure (loosely based on the Boeing 777 structural arrangement) and a new jig outer mold line [97]. The structure and shape were designed to achieve the shape of the original CRM when analyzed using static aeroelastic analysis at the CRM nominal flight condition ($C_L = 0.5$, $M = 0.85$). The benchmark is called the undeflected CRM (uCRM) and has been used in various studies [99,122,123,160].

5. Other applications

The CFD-based optimization efforts are summarized in Table 2. They include the applications that were already mentioned and two other applications that go beyond aircraft applications: the aerodynamic shape optimization of wind turbine blades and the hydrodynamic and hydrostructural optimization of hydrofoils.

While we are not involved in experimental work, we have had two optimization results that have been the subject of experimental measurements. One was the hydrofoil design optimization of Garg et al. [107], which was built and tested in a water tunnel. The experimental results matched the numerical predictions [108]. The other result that was tested was the tow-steered aerostructural optimization of Brooks et al. [99]. Aurora Flight Sciences built a one-third scale model of the optimized wingbox [180] that underwent structural testing at NASA Armstrong Research Center.⁷

6. Conclusions

In this paper, we honor Antony Jameson's legacy by recalling his seminal contributions in the development of the adjoint method. We then review the significant developments of the last decade towards enabling CFD-based aircraft design optimization. The cited references provide much more detail on the methods and their applications. The

common denominator in all of this work is accurate and efficient computation of derivatives via adjoint methods, which, together with gradient-based optimization, enables the solution of large-scale CFD-based aerodynamic shape and MDO for aircraft configurations and other applications. Over the last several years, several challenges were tackled to make the optimization more scalable, robust, and practical. Much of the developed software, including all the components required for aerodynamic shape optimization, are available under an open-source license.⁸

The ADODG benchmark cases motivated many of the reported developments. Even cases that are not realistic from the practical point tested the methods' limits, which ultimately motivated improvements in accuracy and robustness. Exceptions to this are the Euler-based cases, which include issues that we do not think are worth tackling because they disappear when using RANS. Working closely with industry has been invaluable in identifying the challenges that needed to be solved for practical applications.

Given the contributions above and the fact that much of the code that we developed is available under an open-source license, we expect that the use of CFD-based optimization will increase and become more widespread than ever. The recent developments in the OpenMDAO framework, including coupled-adjoint derivative computation, have facilitated the implementation of CFD-based MDO, and we expect further developments in this area.

Jameson's research approach has been remarkable because he was not satisfied with just developing theory; he also put a tremendous effort into implementing his methods through software development and testing those implementations in real-world applications in di-

⁷ The results from this testing have not been published at the time of writing.

⁸ <https://github.com/mdolab/MACH-Aero>

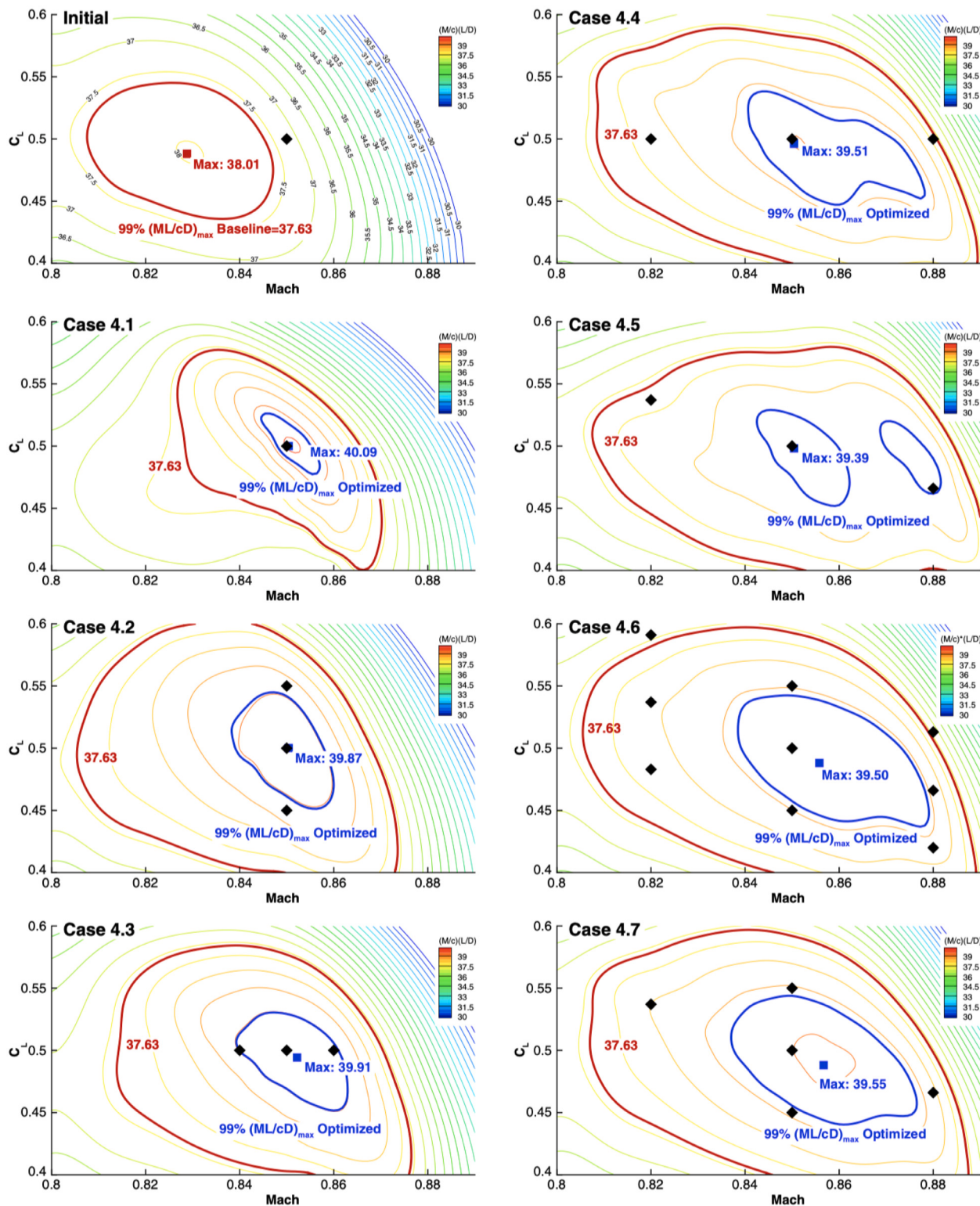


Fig. 16. Aerodynamic performance in the flight condition space for all optimal wings for Case 4 [157].

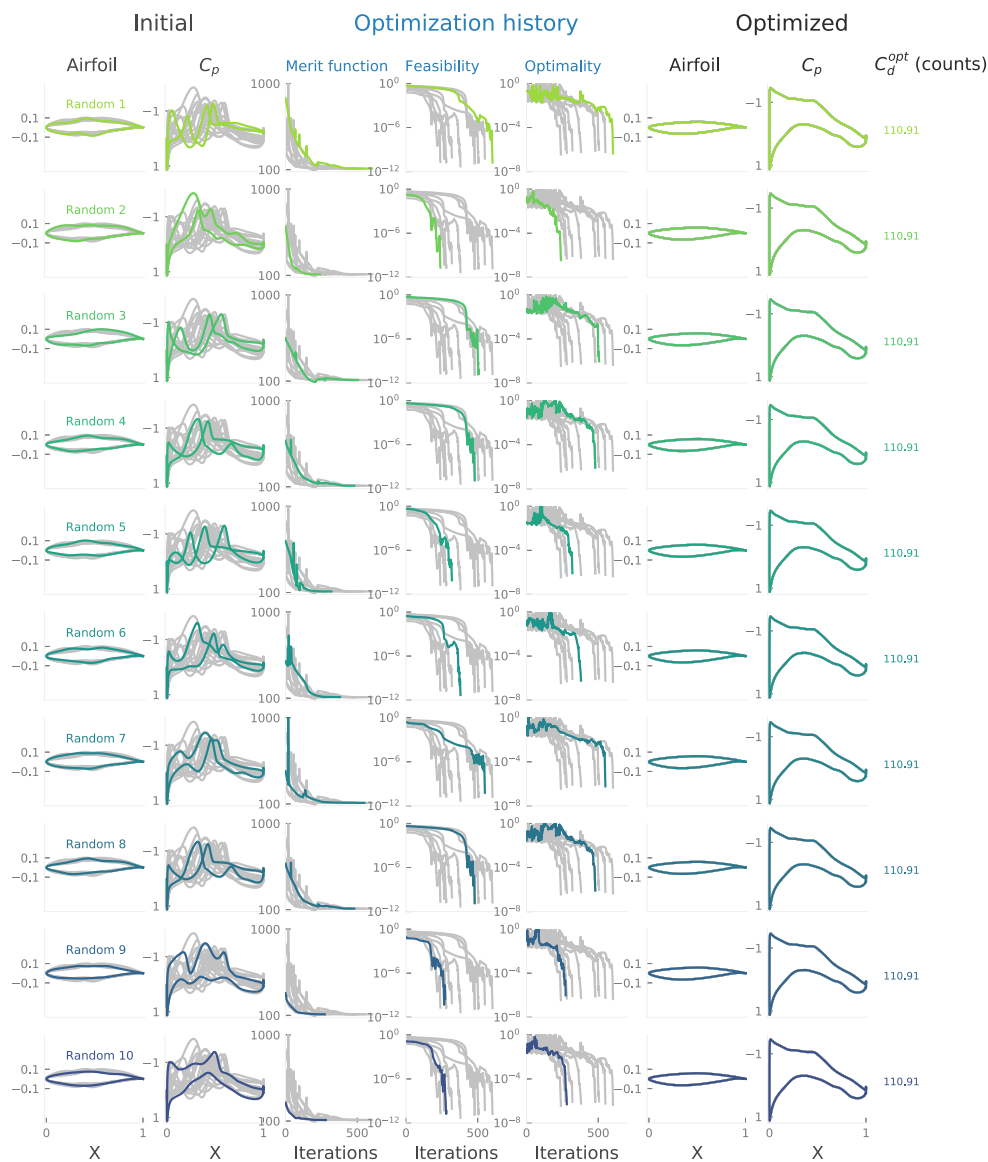


Fig. 17. Optimization starting from 10 random airfoils converged to the same optimal shape [29].

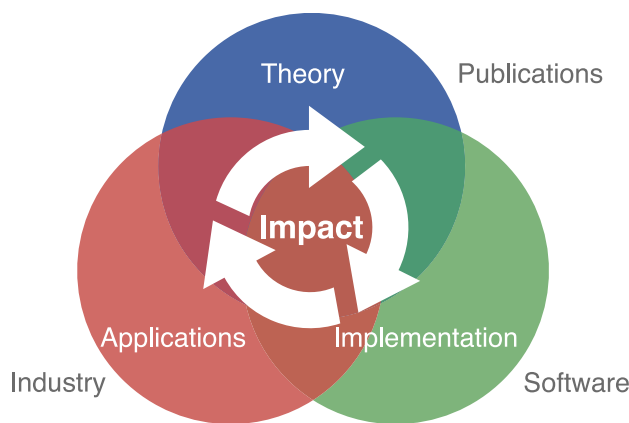


Fig. 18. The circle of impact illustrates the synergies between theory, implementation, and applications.

Source: inspired on a similar figure from a presentation by Antony Jameson.

rect collaborations with industry. The synergy between theory, implementation, and applications is illustrated in Fig. 18. Theory is not enough: Industry usually needs to see a competent implementation and promising results in an application before investing in a new method. Implementation is often undervalued, but implementation details are crucial for computational efficiency and feasibility for practical applications. Finally, practical applications provide insights into the theory that researchers should focus on developing. This research philosophy provides an exemplary model for other researchers to follow that has inspired the author and his research group.

CRediT authorship contribution statement

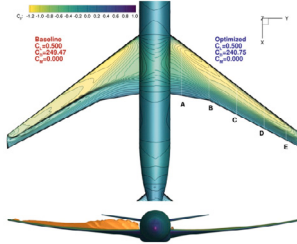
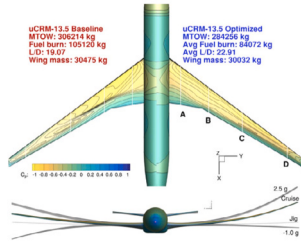
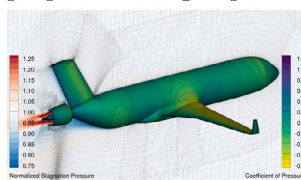
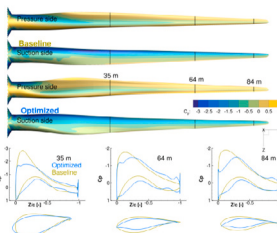
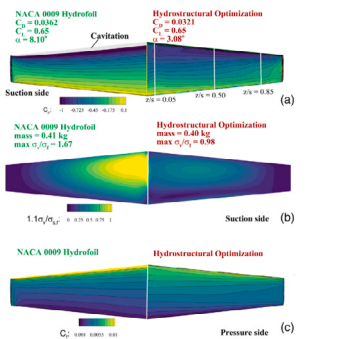
Joaquim R.R.A. Martins: Conceptualization, Resources, Writing – original draft, Writing – review and editing, Project administration, Funding acquisition.

Declaration of competing interest

The authors declare that they have no known competing financial interests or personal relationships that could have appeared to influence the work reported in this paper.

Table 2

List of optimization problems solved with MACH.

Application	References
Aerodynamic shape optimization	2-D transonic aerodynamic shape optimization [29,161] 3-D transonic aerodynamic shape optimization [30,150,157,162] Optimization of novel configurations [163–165] Formulation of buffet constraint for wing design optimization [93] 2-D and 3-D supersonic aerodynamic shape optimization [166] Optimization with spatial integration constraints [167,168] Simultaneous design optimization of shape, trajectory, and aircraft allocation [128]
	
Aerostructural design optimization	Optimization of a transport configuration [97,121,156,169] Optimization with tow-steered composite structures [99,160] Optimization of morphing trailing edge devices [122,123] Optimization with flutter constraints [116,170,171]
	
Aeropropulsive design optimization	Boundary layer ingestion modeling [172] Design optimization of a boundary layer ingestion system [127,173–175]
	
Design optimization of wind turbines	Aerodynamic shape optimization of wind turbine blades [176,177]
	
Optimization of hydrofoils	Hydrodynamic hydrofoil shape optimization [178] Hydrostructural optimization of metallic and composite hydrofoils [107,108,179]
	

Acknowledgments

The author is thankful for the many current and former MDO Lab members who conducted some of the research summarized here: Josh Anibal, Nicolas Bons, Benjamin Brelje, David Burdette, Mohamed Bouhlel, Timothy Brooks, Nitin Garg, Justin Gray, Gustavo Halila, Ping He, Sicheng He, John Hwang, John Jasa, Eirikur Jonsson, Graeme

Kennedy, Gaetan Kenway, Andrew Lambe, Yingqian Liao, Rhea Liem, Zhoujie (Peter) Lyu, Charles Mader, Marco Mangano, Zelu Xu, Anil Yildirim, and Yin Yu. The Webfoil interface was developed by Anjali Balani, Q Cong, and Alan Stahl. Also, some of this work was the result of collaborations with other faculty—William Crossley, Kevin Maki, Yin Lu (Julie) Young, and Frederik Zhale—and visiting students—Song Chen, Tristan Dhert, Xiaolong He, Jichao Li, Mads Madsen, and Yayun

Shi. The cited references contain more detailed information on who contributed to each effort and the funding sources.

Finally, I would like to thank Joël Brezillon for his suggestions.

References

- [1] Slotnick J, Khodadoust A, Alonso J, Darmofal D, Gropp W, Lurie E, Mavriplis D. CFD Vision 2030 Study: A Path to Revolutionary Computational Aerosciences. Technical Report CR-2014-218178, NASA; 2014, URL <https://ntrs.nasa.gov/citations/20140003093>.
- [2] Schulz V, Schillings C. Optimal aerodynamic design under uncertainty. In: Eisfeld B, Barnewitz H, Fritz W, Thiele F, editors. Management and minimisation of uncertainties and errors in numerical aerodynamics: results of the german collaborative project MUNA. Berlin, Heidelberg: Springer Berlin Heidelberg; 2013, p. 297–338. http://dx.doi.org/10.1007/978-3-642-36185-2_13.
- [3] Liem RP, Martins JRRA, Kenway GK. Expected drag minimization for aerodynamic design optimization based on aircraft operational data. *Aerosp Sci Technol* 2017;63:344–62. <http://dx.doi.org/10.1016/j.ast.2017.01.006>.
- [4] Fidkowski KJ, Darmofal DL. Output-based error estimation and mesh adaptation in computational fluid dynamics: Overview and recent results. *AIAA J* 2011a;49(4):673–94.
- [5] Fidkowski KJ, Darmofal DL. Review of output-based error estimation and mesh adaptation in computational fluid dynamics. *AIAA J* 2011b;49(4):673–94. <http://dx.doi.org/10.2514/1.J050073>.
- [6] Chen G, Fidkowski KJ. Discretization error control for constrained aerodynamic shape optimization. *J Comput Phys* 2019;387:163–85. <http://dx.doi.org/10.1016/j.jcp.2019.02.038>.
- [7] Bryson Jr AE. Optimal control—1950 to 1985. *IEEE Control Syst Mag* 1996;16(3):26–33. <http://dx.doi.org/10.1109/37.506395>.
- [8] Arora J, Haug EJ. Methods of design sensitivity analysis in structural optimization. *AIAA J* 1979;17(9):970–4. <http://dx.doi.org/10.2514/3.61260>.
- [9] Pironneau O. On optimum profiles in Stokes flow. *J Fluid Mech* 1973;59(01):117–28. <http://dx.doi.org/10.1017/S002211207300145X>.
- [10] Pironneau O. On optimum design in fluid mechanics. *J Fluid Mech* 1974;64(01):97–110. <http://dx.doi.org/10.1017/S0022112074002023>.
- [11] Jameson A, Ou K. 50 Years of transonic aircraft design. *Prog Aerosp Sci* 2011;47(5):308–18. <http://dx.doi.org/10.1016/j.paerosci.2011.01.001>.
- [12] Jameson A. Automatic design of transonic airfoils to reduce the shock induced pressure drag. In: Proceedings of the 31st Israel annual conference on aviation and aeronautics. Technion-Israel, Haifa, Israel; 1990, p. 5–17.
- [13] Jameson A. Aerodynamic shape optimization using the adjoint method. Von Karman Institute for Fluid Dynamics, Rode Saint Genèse, Belgium; 2003.
- [14] Jameson A. Aerodynamic design via control theory. *J Sci Comput* 1988;3(3):233–60. <http://dx.doi.org/10.1007/BF01061285>.
- [15] Hicks RM, Henne PA. Wing design by numerical optimization. *J Aircr* 1978;15:407–12.
- [16] Jameson A. Computational aerodynamics for aircraft design. *Science* 1989;245:361–71. <http://dx.doi.org/10.1126/science.245.4916.361>.
- [17] Reuther J, Jameson A. A comparison of design variables for control theory based airfoil optimization. IACS Technical Report 95/13, NASA Ames Research Center; 1995.
- [18] Reuther J, Jameson A, Farmer J, Martinelli L, Saunders D. Aerodynamic shape optimization of complex aircraft configurations via an adjoint formulation. In: Proceedings of the 34th AIAA Aerospace Sciences Meeting and exhibit. Reno, Nevada; 1996, AIAA 1996-0094.
- [19] Reuther JJ, Jameson A, Alonso JJ, Rimlinger MJ, Saunders D. Constrained multipoint aerodynamic shape optimization using an adjoint formulation and parallel computers, part 1. *J Aircr* 1999;36(1):51–60.
- [20] Reuther JJ, Jameson A, Alonso JJ, Rimlinger MJ, Saunders D. Constrained multipoint aerodynamic shape optimization using an adjoint formulation and parallel computers, part 2. *J Aircr* 1999;36(1):61–74.
- [21] Jameson A, Martinelli L, Pierce NA. Optimum aerodynamic design using the Navier–Stokes equations. *Theor Comput Fluid Dyn* 1998;10(1–4):213–37. <http://dx.doi.org/10.1007/s001620050060>.
- [22] Anderson WK, Venkatakrishnan V. Aerodynamic design optimization on unstructured grids with a continuous adjoint formulation. *Comput & Fluids* 1999;28(4):443–80. [http://dx.doi.org/10.1016/S0045-7930\(98\)00041-3](http://dx.doi.org/10.1016/S0045-7930(98)00041-3).
- [23] Nielsen EJ, Anderson WK. Aerodynamic design optimization on unstructured meshes using the Navier–Stokes equations. *AIAA J* 1999;37(11):1411–9. <http://dx.doi.org/10.2514/2.640>.
- [24] Jameson A, Martinelli L, Alonso JJ, Vassberg JC, Reuther J. Computational fluid dynamics for the 21st century. Berlin, Heidelberg: Springer; 2001, p. 135–78.
- [25] Yildirim A, Kenway GK, Mader CA, Martins JRRA. A Jacobian-free approximate Newton–Krylov startup strategy for RANS simulations. *J Comput Phys* 2019;397:108741. <http://dx.doi.org/10.1016/j.jcp.2019.06.018>.
- [26] Kelley C, Keyes D. Convergence analysis of pseudo-transient continuation. *SIAM J Numer Anal* 1998;35(2):508–23. <http://dx.doi.org/10.1137/S0036142996304796>.
- [27] Mader CA, Kenway GK, Yildirim A, Martins JRRA. ADflow: An Open-source computational fluid dynamics solver for aerodynamic and multidisciplinary optimization. *J Aerosp Inf Syst* 2020;17(9):508–27.
- [28] Burgess N, Glasby RS. Advances in numerical methods for CREATE-AV analysis tools. In: 52nd Aerospace Sciences Meeting. AIAA SciTech forum, American Institute of Aeronautics and Astronautics; 2014, <http://dx.doi.org/10.2514/6.2014-0417>.
- [29] He X, Li J, Mader CA, Yildirim A, Martins JRRA. Robust aerodynamic shape optimization—from a circle to an airfoil. *Aerosp Sci Technol* 2019;87:48–61. <http://dx.doi.org/10.1016/j.ast.2019.01.051>.
- [30] Lyu Z, Kenway GK, Martins JRRA. Aerodynamic shape optimization investigations of the common research model wing benchmark. *AIAA J* 2015;53(4):968–85. <http://dx.doi.org/10.2514/1.J053318>.
- [31] Martins JRRA, Ning A. Engineering Design Optimization. Cambridge University Press; 2021, <http://dx.doi.org/10.1017/9781108980647>, URL <https://mdobook.github.io>.
- [32] Lyu Z, Xu Z, Martins JRRA. Benchmarking optimization algorithms for wing aerodynamic design optimization. In: Proceedings of the 8th international conference on computational fluid dynamics. Chengdu, Sichuan, China; 2014, ICCFD8-2014-0203.
- [33] Pulliam TH, Nemec M, Holst T, Zingg DW. Comparison of evolutionary (genetic) algorithm and adjoint methods for multi-objective viscous airfoil optimizations. In: Proceedings of the 41st AIAA Aerospace Sciences Meeting and exhibit. Reno, NV; 2003.
- [34] Gill PE, Murray W, Saunders MA. SNOPT: An SQP algorithm for large-scale constrained optimization. *SIAM Rev* 2005;47(1):99–131. <http://dx.doi.org/10.1137/S0036144504446096>.
- [35] Wu N, Kenway G, Mader CA, Jasa J, Martins JRRA. pyOptSparse: a Python framework for large-scale constrained nonlinear optimization of sparse systems. *J. Open Source Software* 2020;5(54):2564. <http://dx.doi.org/10.21105/joss.02564>.
- [36] Nadarajah S, Jameson A. A comparison of the continuous and discrete adjoint approach to automatic aerodynamic optimization. In: Proceedings of the 38th AIAA Aerospace Sciences Meeting and exhibit. Reno, NV; 2000, <http://dx.doi.org/10.2514/6.2000-667>.
- [37] Giles MB, Pierce NA. An introduction to the adjoint approach to design. *Flow Turbul Combust* 2000;65:393–415. <http://dx.doi.org/10.1023/A:1011430410075>.
- [38] Giles MB, Duta MC, Müller J-D, Pierce NA. Algorithm developments for discrete adjoint methods. *AIAA J* 2003;41(2):198–205. <http://dx.doi.org/10.2514/2.1961>.
- [39] Peter JEV, Dwight RP. Numerical sensitivity analysis for aerodynamic optimization: A survey of approaches. *Comput & Fluids* 2010;39(3):373–91. <http://dx.doi.org/10.1016/j.compfluid.2009.09.013>.
- [40] Kenway GK, Mader CA, He P, Martins JRRA. Effective adjoint approaches for computational fluid dynamics. *Prog Aerosp Sci* 2019;110:100542. <http://dx.doi.org/10.1016/j.paerosci.2019.05.002>.
- [41] He P, Mader CA, Martins JRRA, Maki KJ. An aerodynamic design optimization framework using a discrete adjoint approach with OpenFOAM. *Comput & Fluids* 2018;168:285–303. <http://dx.doi.org/10.1016/j.compfluid.2018.04.012>.
- [42] He P, Mader CA, Martins JRRA, Maki KJ. DAFoam multidisciplinary design optimization setup. Mendeley Data; 2019, <http://dx.doi.org/10.17632/cg4n68bm9v>.
- [43] Albring TA, Sagebaum M, Gauger NR. Efficient aerodynamic design using the discrete adjoint method in SU2. In: 17th AIAA/ISSMO multidisciplinary analysis and optimization conference. 2016, p. 3518. <http://dx.doi.org/10.2514/6.2016-3518>.
- [44] Müller J-D, Mykhavskiy O, Hückelheim J. STAMPS: a finite-volume solver framework for adjoint codes derived with source-transformation AD. In: AIAA Multidisciplinary Analysis and Optimization Conference. 2018, <http://dx.doi.org/10.2514/6.2018-2928>.
- [45] Lambe AB, Martins JRRA. Extensions to the design structure matrix for the description of multidisciplinary design, analysis, and optimization processes. *Struct Multidisip Optim* 2012;46:273–84. <http://dx.doi.org/10.1007/s00158-012-0763-y>.
- [46] Brezillon J, Ronzheimer A, Haar D, Abu-Zurayk M, Lummer K, Krugér W, Nattere FJ. Development and application of multi-disciplinary optimization capabilities based on high-fidelity methods. In: 53rd AIAA/ASME/ASCE/AHS/ASC Structures, Structural Dynamics, and Materials Conference. Honolulu, HI; 2012, AIAA 2012-1757.
- [47] Alonso JJ, Martins JRRA, Reuther JJ, Haimes R. High-fidelity aero-structural design using a parametric CAD-based model. In: Proceedings of the 16th AIAA Computational Fluid Dynamics Conference. Orlando, FL; 2003, <http://dx.doi.org/10.2514/6.2003-3429>, AIAA 2003-3429.
- [48] Truong AH, Zingg DW, Haimes R. Surface mesh movement algorithm for computer-aided-design-based aerodynamic shape optimization. *AIAA J* 2016;54(2):542–56. <http://dx.doi.org/10.2514/1.J054295>.
- [49] Dannenhoffer J, Haimes R. Design sensitivity calculations directly on CAD-based geometry. In: 53rd AIAA Aerospace Sciences Meeting. AIAA SciTech forum, American Institute of Aeronautics and Astronautics; 2015, <http://dx.doi.org/10.2514/6.2015-1370>.

- [50] Xu S, Timme S, Mykhaskiv O, Müller J-D. Wing-body junction optimisation with CAD-based parametrisation including a moving intersection. *Aerosp Sci Technol* 2017;68:543–51. <http://dx.doi.org/10.1016/j.ast.2017.06.014>.
- [51] Agarwal D, Robinson TT, Armstrong CG, Marques Sa, Vasilopoulos I, Meyer M. Parametric design velocity computation for CAD-based design optimization using adjoint methods. *Eng Comput* 2018;34(2):225–39. <http://dx.doi.org/10.1007/s00366-017-0534-x>.
- [52] Mykhaskiv O, Banović M, Auriemma S, Mohanamurly P, Walther A, Legrand H, Müller J-D. NURBS-Based and parametric-based shape optimization with differentiated CAD kernel. *Comput-Aided Des Appl* 2018;15(6):916–26. <http://dx.doi.org/10.1080/16864360.2018.1462881>.
- [53] Banović M, Mykhaskiv O, Auriemma S, Walther A, Legrand H, Müller J-D. Algorithmic differentiation of the open CASCADE technology CAD kernel and its coupling with an adjoint CFD solver. *Optim Methods Softw* 2018;33(4–6):813–28. <http://dx.doi.org/10.1080/10556788.2018.1431235>.
- [54] Kenway GKW, Kennedy GJ, Martins JRRA. A CAD-free approach to high-fidelity aerostructural optimization. In: Proceedings of the 13th AIAA/ISSMO Multidisciplinary Analysis Optimization Conference. AIAA 2010-9231. Fort Worth, TX; 2010, <http://dx.doi.org/10.2514/6.2010-9231>.
- [55] Hicken JE, Zingg DW. Aerodynamic optimization algorithm with integrated geometry parameterization and mesh movement. *AIAA J* 2010;48(2):400–13. <http://dx.doi.org/10.2514/1.44033>.
- [56] Samareh JA. Survey of shape parameterization techniques for high-fidelity multidisciplinary shape optimization. *AIAA J* 2001;39(5):877–84. <http://dx.doi.org/10.2514/2.1391>.
- [57] Castonguay P, Nadarajah SK. Effect of shape parameterization on aerodynamic shape optimization. In: 45th AIAA Aerospace Sciences Meeting. Reno, Nevada; 2007, <http://dx.doi.org/10.2514/6.2007-59>.
- [58] Lee C, Koo D, Zingg DW. Comparison of B-spline surface and free-form deformation geometry control for aerodynamic optimization. *AIAA J* 2017;55(1):228–40. <http://dx.doi.org/10.2514/1.J055102>.
- [59] Masters DA, Taylor NJ, Rendall TCS, Allen CB, Poole DJ. Geometric comparison of airfoil shape parameterization methods. *AIAA J* 2017;55(5):1575–89. <http://dx.doi.org/10.2514/1.J054943>.
- [60] Rajnarayan D, Ning A, Mehr JA. Universal airfoil parametrization using B-splines. In: Proceedings of the AIAA Aviation Forum. 2018, <http://dx.doi.org/10.2514/6.2018-3949>.
- [61] Secco N, Kenway GK, He P, Mader CA, Martins JRRA. Efficient mesh generation and deformation for aerodynamic shape optimization. *AIAA J* 2021;59(4):1151–68. <http://dx.doi.org/10.2514/1.J059491>.
- [62] Luke E, Collins E, Blades E. A fast mesh deformation method using explicit interpolation. *J Comput Phys* 2012;231(2):586–601. <http://dx.doi.org/10.1016/j.jcp.2011.09.021>.
- [63] Economou TD, Palacios F, Copeland SR, Lukaczyk TW, Alonso JJ. SU2: AN open-source suite for multiphysics simulation and design. *AIAA J* 2016;54(3):828–46. <http://dx.doi.org/10.2514/1.J053813>.
- [64] Hahn A. Vehicle sketch pad: A parametric geometry modeler for conceptual aircraft design. In: 48th AIAA Aerospace Sciences Meeting including the new horizons forum and aerospace exposition. Aerospace sciences meetings, American Institute of Aeronautics and Astronautics; 2010, <http://dx.doi.org/10.2514/6.2010-657>.
- [65] Li J, Bouhlel MA, Martins JRRA. Data-based approach for fast airfoil analysis and optimization. *AIAA J* 2019;57(2):581–96. <http://dx.doi.org/10.2514/1.J057129>.
- [66] Li J, He S, Martins JRRA. Data-driven constraint approach to ensure low-speed performance in transonic aerodynamic shape optimization. *Aerosp Sci Technol* 2019;92:536–50. <http://dx.doi.org/10.1016/j.ast.2019.06.008>.
- [67] Brelje BJ, Anibal J, Yildirim A, Mader CA, Martins JRRA. Flexible formulation of spatial integration constraints in aerodynamic shape optimization. *AIAA J* 2020;58(6):2571–80. <http://dx.doi.org/10.2514/1.J058366>.
- [68] Brelje BJ, Martins JRRA. Aerostructural wing optimization for a hydrogen fuel cell aircraft. In: Proceedings of the AIAA SciTech forum. 2021, <http://dx.doi.org/10.2514/6.2021-1132>.
- [69] Fu S, Wang L. RANS Modeling of high-speed aerodynamic flow transition with consideration of stability theory. *Prog Aerosp Sci* 2013;58:36–59. <http://dx.doi.org/10.1016/j.paerosci.2012.08.004>.
- [70] Krishnan KS, Bertram O, Seibel O. Review of hybrid laminar flow control systems. *Prog Aerosp Sci* 2017;93:24–52. <http://dx.doi.org/10.1016/j.paerosci.2017.05.005>.
- [71] Coder JG, Hue D, Kenway G, Pulliam TH, Sclafani AJ, Serrano L, Vassberg JC. Contributions to the sixth drag prediction workshop using structured, overset grid methods. *J Aircr* 2018;55(4):1406–19. <http://dx.doi.org/10.2514/1.C034486>.
- [72] Arnal D, Casalis G. Laminar-turbulent transition prediction in three-dimensional flows. *Prog Aerosp Sci* 2000;36(2):173–91. [http://dx.doi.org/10.1016/S0376-0421\(00\)00002-6](http://dx.doi.org/10.1016/S0376-0421(00)00002-6).
- [73] Halila GLO, Chen G, Shi Y, Fidkowski KJ, Martins JRRA, de Mendonça MT. High-Reynolds number transitional flow simulation via parabolized stability equations with an adaptive RANS solver. *Aerosp Sci Technol* 2019;91:321–36. <http://dx.doi.org/10.1016/j.ast.2019.05.018>.
- [74] Halila GLO, Fidkowski KJ, Martins JRRA. Toward automatic parabolized stability equation-based transition-to-turbulence prediction for aerodynamic flows. *AIAA J* 2021;59(2):462–73. <http://dx.doi.org/10.2514/1.J059516>.
- [75] Roberto dePompeis PC, Martini PIS. Development and Certification Flight Test on the Piaggio P.180 Avanti Aircraft: A General Overview. SAE Technical Paper 911003, SAE International; 1991, <http://dx.doi.org/10.4271/911003>.
- [76] Fujino M, Yoshizaki Y, Kawamura Y. Natural-laminar-flow airfoil development for a lightweight business jet. *J Aircr* 2003;40(4):609–15. <http://dx.doi.org/10.2514/2.3145>.
- [77] Crouch J. Modeling transition physics for laminar flow control. In: Proceedings of the 38th Fluid Dynamics Conference. AIAA; 2008, <http://dx.doi.org/10.2514/6.2008-3832>.
- [78] Langtry RB, Menter FR. Correlation-based transition modeling for unstructured parallelized computational fluid dynamics codes. *AIAA J* 2009;47(12):2894–906. <http://dx.doi.org/10.2514/1.42362>.
- [79] Khayatzadeh P, Nadarajah S. Aerodynamic shape optimization of natural laminar flow (NLF) airfoils. In: 50th AIAA Aerospace Sciences Meeting including the new horizons forum and aerospace exposition. 2012, p. 1–15. <http://dx.doi.org/10.2514/6.2012-61>.
- [80] Grabe C, Shengyang N, Krumbein A. Transport modeling for the prediction of crossflow transition. *AIAA J* 2018;56(8):3167–78. <http://dx.doi.org/10.2514/1.j056200>.
- [81] Choi JH, Kwon OJ. Enhancement of a correlation-based transition turbulence model for simulating crossflow instability. *AIAA J* 2015;53(10):3063–72. <http://dx.doi.org/10.2514/1.J053887>.
- [82] Khayatzadeh P, Nadarajah S. Aerodynamic shape optimization via discrete viscous adjoint equations for the $k-\omega$ SST turbulence and $\gamma - Re_\theta$ transition models. In: Proceedings of the 49th AIAA Aerospace Sciences Meeting including the new horizons forum and aerospace exposition. Orlando, FL; 2011, <http://dx.doi.org/10.2514/6.2011-1247>.
- [83] Halila GLO, Martins JRRA, Fidkowski KJ. Adjoint-based aerodynamic shape optimization including transition to turbulence effects. *Aerosp Sci Technol* 2020;107:1–15. <http://dx.doi.org/10.1016/j.ast.2020.106243>.
- [84] Wang G, Mian HH, Ye Z-Y, Lee J-D. Numerical study of transitional flow around NLR-7301 airfoil using correlation-based transition model. *J Aircr* 2014;51(1):342–50. <http://dx.doi.org/10.2514/1.C032063>.
- [85] Coder JG, Maughmer MD. Computational fluid dynamics compatible transition modeling using an amplification factor transport equation. *AIAA J* 2014;52(11):2506–12. <http://dx.doi.org/10.2514/1.J052905>.
- [86] Grabe C, Krumbein A. Correlation-based transition transport modeling for three-dimensional aerodynamic configurations. *J Aircr* 2013;50(5). <http://dx.doi.org/10.2514/1.C032063>.
- [87] Amoignon OG, Pralits JO, Hanifi A, Berggren M, Henningson DS. Shape optimization for delay of laminar-turbulent transition. *AIAA J* 2006;44(5):1009–24. <http://dx.doi.org/10.2514/1.12431>.
- [88] Driver J, Zingg DW. Numerical aerodynamic optimization incorporating laminar-turbulent transition prediction. *AIAA J* 2007;45(8):1810–8. <http://dx.doi.org/10.2514/1.23569>.
- [89] Rashad R, Zingg DW. Aerodynamic shape optimization for natural laminar flow using a discrete-adjoint approach. *AIAA J* 2016;54(11):3321–37. <http://dx.doi.org/10.2514/1.J054940>.
- [90] Perraud J, Arnal D, Casalis G, Archambaud J-P, Donelli R. Automatic transition predictions using simplified methods. *AIAA J* 2009;47(11):2676–84. <http://dx.doi.org/10.2514/1.42990>.
- [91] Shi Y, Mader CA, He S, Halila GLO, Martins JRRA. Natural laminar-flow airfoil optimization design using a discrete adjoint approach. *AIAA J* 2020;58(11):4702–22. <http://dx.doi.org/10.2514/1.J058944>.
- [92] Shi Y, Mader CA, Martins JRRA. Natural laminar flow wing optimization using a discrete adjoint approach. *Struct Multidiscip Optim* 2021;64:541–62. <http://dx.doi.org/10.1007/s0158-021-02936-w>.
- [93] Kenway GK, Martins JRRA. Buffet-onset constraint formulation for aerodynamic shape optimization. *AIAA J* 2017;55(6):1930–47. <http://dx.doi.org/10.2514/1.J055172>.
- [94] Kenway GK, Martins JRRA. High-fidelity aerostructural optimization considering buffet onset. In: Proceedings of the 16th AIAA/ISSMO Multidisciplinary Analysis and Optimization Conference. Dallas, TX; 2015, AIAA 2015-2790.
- [95] Kenway GK, Martins JRRA. Aerodynamic shape optimization of the CRM configuration including buffet-onset conditions. In: 54th AIAA Aerospace Sciences Meeting. San Diego, CA: American Institute of Aeronautics and Astronautics; 2016, <http://dx.doi.org/10.2514/6.2016-1294>.
- [96] Mader CA, Kenway GK, Martins JRRA, Uranga A. Aerostructural optimization of the D8 wing with varying cruise mach numbers. In: 18th AIAA/ISSMO multidisciplinary analysis and optimization conference. American Institute of Aeronautics and Astronautics; 2017, <http://dx.doi.org/10.2514/6.2017-4436>.
- [97] Brooks TR, Kenway GK, Martins JRRA. Benchmark aerostructural models for the study of transonic aircraft wings. *AIAA J* 2018;56(7):2840–55. <http://dx.doi.org/10.2514/1.J056603>.
- [98] Bons N, Martins JRRA, Odaguil F, Cuco APC. Aerostructural wing optimization of a regional jet considering mission fuel burn. *ASME Open Journal of Engineering* 2022. (In press).

- [99] Brooks TR, Martins JRRA, Kennedy GJ. High-fidelity aerostructural optimization of tow-steered composite wings. *J Fluids Struct* 2019;88:122–47. <http://dx.doi.org/10.1016/j.jfluidstructs.2019.04.005>.
- [100] Balakrishna S, Acheson M. Analysis of NASA common research model dynamic data. In: 49th Aerospace Sciences Meeting. 2011, <http://dx.doi.org/10.2514/6.2011-1127>.
- [101] Giannelis NF, Vio GA, Levinski O. A review of recent developments in the understanding of transonic shock buffet. *Prog Aerosp Sci* 2017;92:39–84. <http://dx.doi.org/10.1016/j.paerosci.2017.05.004>.
- [102] Raveh DE, Dowell EH. Frequency lock-in phenomenon for oscillating airfoils in buffeting flows. *J Fluids Struct* 2011;27(1):89–104. <http://dx.doi.org/10.1016/j.jfluidstructs.2010.10.001>.
- [103] Thomas J, Dowell E. Discrete adjoint design optimization approach for increasing transonic buffet onset angle-of-attack. In: 16th AIAA/ISSMO multidisciplinary analysis and optimization conference. American Institute of Aeronautics and Astronautics; 2015, <http://dx.doi.org/10.2514/6.2015-3435>.
- [104] Crouch JD, Garbaruk A, Strelets M. Global instability in the onset of transonic-wing buffet. *J Fluid Mech* 2019;881:3–22.
- [105] Timme S. Global instability of wing shock-buffet onset. *J Fluid Mech* 2020;885:A37. <http://dx.doi.org/10.1017/jfm.2019.1001>.
- [106] Bons NP, Martins JRRA. Aerostructural design exploration of a wing in transonic flow. *Aerospace* 2020;7(8):118. <http://dx.doi.org/10.3390/aerospace7080118>.
- [107] Garg N, Kenway GKW, Martins JRRA, Young YL. High-fidelity multipoint hydrostructural optimization of a 3-D hydrofoil. *J Fluids Struct* 2017;71:15–39. <http://dx.doi.org/10.1016/j.jfluidstructs.2017.02.001>.
- [108] Garg N, Pearce BW, Brandner PA, Phillips AW, Martins JRRA, Young YL. Experimental investigation of a hydrofoil designed via hydrostructural optimization. *J Fluids Struct* 2019;84:243–62. <http://dx.doi.org/10.1016/j.jfluidstructs.2018.10.010>.
- [109] Jonsson E, Riso C, Lupp CA, Cesnik CES, Martins JRRA, Epureanu BI. Flutter and post-flutter constraints in aircraft design optimization. *Prog Aerosp Sci* 2019;109:100537. <http://dx.doi.org/10.1016/j.paerosci.2019.04.001>.
- [110] Livne E, Li W-L. Aeroversoelastic aspects of wing/control surface planform shape optimization. *AAIA J* 1995;33(2):302–11. <http://dx.doi.org/10.2514/3.12482>.
- [111] Stanford B, Beran P. Direct flutter and limit cycle computations of highly flexible wings for efficient analysis and optimization. *J Fluids Struct* 2013;36:111–23. <http://dx.doi.org/10.1016/j.jfluidstructs.2012.08.008>.
- [112] Townsend S, Picelli R, Stanford B, Kim HA. Structural optimization of platelike aircraft wings under flutter and divergence constraints. In: AIAA Journal. AIAA J 2018;56(8):3307–19. <http://dx.doi.org/10.2514/1.J056748>.
- [113] Bartels RE, Stanford BK. Aeroelastic optimization with an economical transonic flutter constraint using Navier-Stokes aerodynamics. *J Aircr* 2018;55(4):1522–30. <http://dx.doi.org/10.2514/1.C034675>.
- [114] Jonsson E, Mader CA, Kennedy GJ, Martins JRRA. Computational modeling of flutter constraint for high-fidelity aerostructural optimization. In: AIAA/ASCE/AHS/ASC Structures, Structural Dynamics, and Materials Conference. San Diego, CA: American Institute of Aeronautics and Astronautics; 2019, <http://dx.doi.org/10.2514/6.2019-2354>.
- [115] Jacobson KE, Kiviaho JF, Kennedy GJ, Smith MJ. Evaluation of time-domain damping identification methods for flutter-constrained optimization. *J Fluids Struct* 2019;87:174–88. <http://dx.doi.org/10.1016/j.jfluidstructs.2019.03.011>.
- [116] He S, Jonsson E, Mader CA, Martins JRRA. A coupled Newton-Krylov time-spectral solver for wing flutter and LCO prediction. In: AIAA Aviation Forum. Dallas, TX; 2019, <http://dx.doi.org/10.2514/6.2019-3549>.
- [117] He S, Jonsson E, Mader CA, Martins JRRA. Coupled newton-krylov time-spectral solver for flutter and limit cycle oscillation prediction. *AAIA Journal* 2021;59(6):2214–32. <http://dx.doi.org/10.2514/1.J059224>.
- [118] Martins JRRA, Lambe AB. Multidisciplinary design optimization: A survey of architectures. *AAIA J* 2013;51(9):2049–75. <http://dx.doi.org/10.2514/1.J051895>.
- [119] Kenway GKW, Kennedy GJ, Martins JRRA. Scalable parallel approach for high-fidelity steady-state aeroelastic analysis and adjoint derivative computations. *AAIA J* 2014;52(5):935–51. <http://dx.doi.org/10.2514/1.J052255>.
- [120] Kennedy GJ, Martins JRRA. A parallel finite-element framework for large-scale gradient-based design optimization of high-performance structures. *Finite Elem Anal Des* 2014;87:56–73. <http://dx.doi.org/10.1016/j.finel.2014.04.011>.
- [121] Liem RP, Kenway GKW, Martins JRRA. Multimission aircraft fuel burn minimization via multipoint aerostructural optimization. *AAIA J* 2015;53(1):104–22. <http://dx.doi.org/10.2514/1.J052940>.
- [122] Burdette DA, Martins JRRA. Design of a transonic wing with an adaptive morphing trailing edge via aerostructural optimization. *Aerosp Sci Technol* 2018;81:192–203. <http://dx.doi.org/10.1016/j.ast.2018.08.004>.
- [123] Burdette DA, Martins JRRA. Impact of morphing trailing edge on mission performance for the common research model. *J Aircr* 2019;56(1):369–84. <http://dx.doi.org/10.2514/1.C034967>.
- [124] Martins JRRA, Hwang JT. Review and unification of methods for computing derivatives of multidisciplinary computational models. *AAIA J* 2013;51(11):2582–99. <http://dx.doi.org/10.2514/1.J052184>.
- [125] Hwang JT, Martins JRRA. A computational architecture for coupling heterogeneous numerical models and computing coupled derivatives. *ACM Trans Math Software* 2018;44(4):37. <http://dx.doi.org/10.1145/3182393>.
- [126] Gray JS, Hwang JT, Martins JRRA, Moore KT, Naylor BA. OpenMDAO: An open-source framework for multidisciplinary design, analysis, and optimization. *Struct Multidiscip Optim* 2019;59(4):1075–104. <http://dx.doi.org/10.1007/s00158-019-02211-z>.
- [127] Gray JS, Martins JRRA. Coupled aeropropulsive design optimization of a boundary-layer ingestion propulsor. *Aeronaut J* 2019;123(1259):121–37. <http://dx.doi.org/10.1017/aer.2018.120>.
- [128] Hwang JT, Jasa J, Martins JRRA. High-fidelity design-allocation optimization of a commercial aircraft maximizing airline profit. *J Aircr* 2019;56(3):1165–78. <http://dx.doi.org/10.2514/1.C035082>.
- [129] Roy S, Crossley WA, Moore KT, Gray JS, Martins JRRA. Monolithic approach towards next generation aircraft design considering airline operations and economics. *J Aircr* 2019;56(4):1565–76. <http://dx.doi.org/10.2514/1.C035312>.
- [130] Carrier G, Destarac D, Dumont A, Méheut M, Din ISE, Peter J, Khelil SB, Brezillon J, Pestana M. Gradient-based aerodynamic optimization with the *elsA* software. In: 52nd Aerospace Sciences Meeting. 2014, <http://dx.doi.org/10.2514/6.2014-0568>.
- [131] Telidetzki K, Osusky L, Zingg DW. Application of jetstream to a suite of aerodynamic shape optimization problems. In: 52nd Aerospace Sciences Meeting. 2014, <http://dx.doi.org/10.2514/6.2014-0571>.
- [132] Anderson GR, Nemec M, Aftosmis MJ. Aerodynamic shape optimization benchmarks with error control and automatic parameterization. In: 53rd AIAA Aerospace Sciences Meeting. 2015, p. 1719. <http://dx.doi.org/10.2514/6.2015-1719>.
- [133] Bisson F, Nadarajah. Adjoint-based aerodynamic optimization of benchmark problems. In: 53rd Aerospace Sciences Meeting. 2015, <http://dx.doi.org/10.2514/6.2015-1948>.
- [134] Tesfahunegn YA, Koziel S, Leifsson L, Bekasiewicz A. Surrogate-based airfoil design with space mapping and adjoint sensitivity. *Procedia Comput Sci* 2015;51:795–804. <http://dx.doi.org/10.1016/j.procs.2015.05.201>, International Conference On Computational Science, ICCS 2015.
- [135] LeDoux ST, Vassberg JC, Young DP, Fugal S, Kamenetskiy D, Huffman WP, Melvin RG, Smith MF. Study based on the AIAA aerodynamic design optimization discussion group test cases. *AAIA J* 2015;53:1910–35. <http://dx.doi.org/10.2514/1.j053535>.
- [136] Lee C, Koo D, Telidetzki K, Buckley H, Gagnon H, Zingg DW. Aerodynamic shape optimization of benchmark problems using jetstream. In: Proceedings of the 53rd AIAA Aerospace Sciences Meeting. American Institute of Aeronautics and Astronautics (AIAA); 2015, <http://dx.doi.org/10.2514/6.2015-0262>.
- [137] Gariepy M, Trenepier J-Y, Malouin B, Tribes C. Direct search airfoil optimization using far-field drag decomposition results. In: 53rd AIAA Aerospace Sciences Meeting. 2015, <http://dx.doi.org/10.2514/6.2015-1720>.
- [138] Poole DJ, Allen CB, Rendall T. Control point-based aerodynamic shape optimization applied to AAIA ADODG test cases. In: 53rd AIAA Aerospace Sciences Meeting. 2015.
- [139] Ren J, Thelen A, Amrit A, Du X, Leifsson L, Tesfahunegn YA, Koziel S. Application of multi fidelity optimization techniques to benchmark aerodynamic design problems. In: AIAA Aviation Forum. San Diego, CA; 2016, <http://dx.doi.org/10.2514/6.2016-1542>.
- [140] Zhang Y, Han Z-H, Shi L, Song W-P. Multi-round surrogate-based optimization for benchmark aerodynamic design problems. In: 54th AIAA Aerospace Sciences Meeting. 2016, p. 1545. <http://dx.doi.org/10.2514/6.2016-1545>.
- [141] Fabiano E, Mavriplis D. Adjoint-based aerodynamic design on unstructured meshes. In: 54nd Aerospace Sciences Meeting. 2016, <http://dx.doi.org/10.2514/6.2016-1295>.
- [142] Masters DA, Poole DJ, Taylor NJ, Rendall T, Allen CB. Impact of shape parameterisation on aerodynamic optimisation of benchmark problems. In: 54rd AIAA Aerospace Sciences Meeting. 2016, <http://dx.doi.org/10.2514/6.2016-1544>.
- [143] Masters D, Taylor N, Rendall T, Allen C. Multilevel subdivision parameterization scheme for aerodynamic shape optimization. *AAIA J* 2017;1–16. <http://dx.doi.org/10.2514/1.J055785>.
- [144] Amrit A, Du X, Thelen A, Leifsson L, Koziel S. Surrogate-based optimization applied to benchmark aerodynamic design problems. In: AIAA Aviation Forum. Denver, CO; 2017, <http://dx.doi.org/10.2514/6.2017-4367>.
- [145] Destarac D, Carrier G, Anderson GR, Nadarajah S, Poole DJ, Vassberg JC, Zingg DW. Example of a pitfall in aerodynamic shape optimization. *AAIA J* 2018;56(4):1532–40. <http://dx.doi.org/10.2514/1.J056128>.
- [146] Amrit A, Du X, Thelen A, Leifsson L, Koziel S. Aerodynamic design of the RAE 2822 in transonic viscous flow: Single- and multi-objective optimization studies. In: AIAA Aviation Forum. Denver, CO; 2017, <http://dx.doi.org/10.2514/6.2017-3751>.
- [147] Méheut M, Dumont A, Carrier G, Peter JE. Gradient-based optimization of CRM wing-alone and wing-body-tail configurations by RANS adjoint technique. In: 54th AIAA Aerospace Sciences Meeting. American Institute of Aeronautics and Astronautics; 2016, <http://dx.doi.org/10.2514/6.2016-1293>.

- [148] Shi-Dong D, Chen C-H, Nadarajah S. Adjoint-based aerodynamic optimization of benchmark CRM wing. In: 35th AIAA Applied Aerodynamics Conference. American Institute of Aeronautics and Astronautics; 2017, <http://dx.doi.org/10.2514/6.2017-3755>.
- [149] Yu Y, Lyu Z, Xu Z, Martins JRRA. On the influence of optimization algorithm and starting design on wing aerodynamic shape optimization. *Aerospace Sci Technol* 2018;75:183–99. <http://dx.doi.org/10.1016/j.ast.2018.01.016>.
- [150] Chen S, Lyu Z, Kenway GK, Martins JRRA. Aerodynamic shape optimization of the common research model wing-body-tail configuration. *J Aircr* 2016;53(1):276–93. <http://dx.doi.org/10.2514/1.C033328>.
- [151] Bons NP, He X, Mader CA, Martins JRRA. Multimodality in aerodynamic wing design optimization. *AIAA J* 2019;57(3):1004–18. <http://dx.doi.org/10.2514/1.J057294>.
- [152] Streuber GM, Zingg DW. Investigation of multimodality in aerodynamic shape optimization based on the Reynolds-averaged Navier-Stokes equations. In: Proceedings of the 18th AIAA/ISSMO multidisciplinary analysis and optimization conference. Denver, CO; 2017.
- [153] Lyu Z, Kenway GK, Paige C, Martins JRRA. Automatic differentiation adjoint of the Reynolds-averaged Navier-Stokes equations with a turbulence model. In: 21st AIAA computational fluid dynamics conference. San Diego, CA; 2013, <http://dx.doi.org/10.2514/6.2013-2581>.
- [154] Vuruskan A, Hosder S. Impact of turbulence models and shape parameterization on robust aerodynamic shape optimization. *J Aircr* 2019;56(3):1099–115. <http://dx.doi.org/10.2514/1.C035039>.
- [155] Vuruskan A, Hosder S. Impact of turbulence models on robust aerodynamic shape optimization of 3-D wing geometries. In: Proceedings of the AIAA Scitech 2021 Forum. 2021, <http://dx.doi.org/10.2514/6.2021-0339>.
- [156] Kenway GK, Martins JRRA. Multipoint high-fidelity aerostructural optimization of a transport aircraft configuration. *J Aircr* 2014;51(1):144–60. <http://dx.doi.org/10.2514/1.C032150>.
- [157] Kenway GK, Martins JRRA. Multipoint aerodynamic shape optimization investigations of the common research model wing. *AIAA J* 2016;54(1):113–28. <http://dx.doi.org/10.2514/1.J054154>.
- [158] Martins JRRA, Sturdza P, Alonso JJ. The complex-step derivative approximation. *ACM Trans Math Software* 2003;29(3):245–62. <http://dx.doi.org/10.1145/838250.838251>.
- [159] Vassberg JC, DeHaan MA, Rivers MS, Wahls RA. Retrospective on the common research model for computational fluid dynamics validation studies. *J Aircr* 2018;55(4):1325–37. <http://dx.doi.org/10.2514/1.C034906>.
- [160] Brooks TR, Martins JRRA. On manufacturing constraints for tow-steered composite design optimization. *Compos Struct* 2018;204:548–59. <http://dx.doi.org/10.1016/j.comstruct.2018.07.100>.
- [161] Li J, Bouhlel MA, Martins JRRA. A data-based approach for fast airfoil analysis and optimization. In: 2018 AIAA/ASCE/AHS/ASC Structures, Structural Dynamics, and Materials Conference. Kissimmee, FL; 2018, <http://dx.doi.org/10.2514/6.2018-1383>.
- [162] Lyu Z, Martins JRRA. Aerodynamic shape optimization of an adaptive morphing trailing edge wing. *J Aircr* 2015;52(6):1951–70. <http://dx.doi.org/10.2514/1.C033116>.
- [163] Mader CA, Martins JRRA. Stability-constrained aerodynamic shape optimization of flying wings. *J Aircr* 2013;50(5):1431–49. <http://dx.doi.org/10.2514/1.C031956>.
- [164] Lyu Z, Martins JRRA. Aerodynamic design optimization studies of a blended-wing-body aircraft. *J Aircr* 2014;51(5):1604–17. <http://dx.doi.org/10.2514/1.C032491>.
- [165] Secco NR, Martins JRRA. RANS-Based aerodynamic shape optimization of a strut-braced wing with overset meshes. *J Aircr* 2019;56(1):217–27. <http://dx.doi.org/10.2514/1.C034934>.
- [166] Mangano M, Martins JRRA. Multipoint aerodynamic shape optimization for subsonic and supersonic regimes. In: 57th AIAA Aerospace Sciences Meeting, AIAA SciTech forum, 2019. San Diego, CA; 2019, <http://dx.doi.org/10.2514/6.2019-0696>.
- [167] Brelje BJ, Martins JRRA. Coupled component sizing and aerodynamic shape optimization via geometric constraints. In: AIAA Aviation Forum. Dallas, TX: American Institute of Aeronautics and Astronautics; 2019, <http://dx.doi.org/10.2514/6.2019-3105>.
- [168] Brelje BJ, Anibal JL, Yildirim A, Mader CA, Martins JRRA. Flexible formulation of spatial integration constraints in aerodynamic shape optimization. In: 57th AIAA Aerospace Sciences Meeting, AIAA SciTech forum. San Diego, CA; 2019, <http://dx.doi.org/10.2514/6.2019-2355>.
- [169] Bons NP, Martins JRRA. Aerostructural wing design exploration with multidisciplinary design optimization. In: Proceedings of the AIAA SciTech forum. Orlando, FL; 2020, <http://dx.doi.org/10.2514/6.2020-0544>.
- [170] He S, Jonsson E, Mader CA, Martins JRRA. Aerodynamic shape optimization with time spectral flutter adjoint. In: 2019 AIAA/ASCE/AHS/ASC Structures, Structural Dynamics, and Materials Conference. San Diego, CA: American Institute of Aeronautics and Astronautics; 2019, <http://dx.doi.org/10.2514/6.2019-0697>.
- [171] He S, Jonsson E, Mader CA, Martins JRRA. A coupled Newton-Krylov time spectral solver for flutter prediction. In: 2018 AIAA/ASCE/AHS/ASC structures, structural dynamics, and materials conference. Kissimmee, FL: American Institute of Aeronautics and Astronautics; 2018, <http://dx.doi.org/10.2514/6.2018-2149>.
- [172] Gray JS, Mader CA, Kenway GK, Martins JRRA. Modeling boundary layer ingestion using a coupled aeropropulsive analysis. *J Aircr* 2018;55(3):1191–9. <http://dx.doi.org/10.2514/1.C034601>.
- [173] Yildirim A, Gray JS, Mader CA, Martins JRRA. Aeropropulsive design optimization of a boundary layer ingestion system. In: AIAA Aviation Forum. Dallas, TX; 2019, <http://dx.doi.org/10.2514/6.2019-3455>.
- [174] Gray JS, Kenway GK, Mader CA, Martins JRRA. Aero-propulsive design optimization of a turboelectric boundary layer ingestion propulsion system. In: 2018 AIAA/ISSMO multidisciplinary analysis and optimization conference. Atlanta, GA; 2018, <http://dx.doi.org/10.2514/6.2018-3976>, AIAA 2018-3976.
- [175] Kenway GK, Kiris CC. Aerodynamic shape optimization of the STAR-CABL concept for minimal inlet distortion. In: AIAA/ASCE/AHS/ASC structures, structural dynamics, and materials conference. American Institute of Aeronautics and Astronautics; 2018, <http://dx.doi.org/10.2514/6.2018-1912>.
- [176] Madsen MHA, Zahle F, Sørensen NN, Martins JRRA. Multipoint high-fidelity CFD-based aerodynamic shape optimization of a 10 MW wind turbine. *Wind Energy Sci* 2019;4:163–92. <http://dx.doi.org/10.5194/wes-4-163-2019>.
- [177] Dhert T, Ashuri T, Martins JRRA. Aerodynamic shape optimization of wind turbine blades using a Reynolds-averaged Navier-Stokes model and an adjoint method. *Wind Energy* 2017;20(5):909–26. <http://dx.doi.org/10.1002/we.2070>.
- [178] Garg N, Kenway GK, Lyu Z, Martins JRRA, Young YL. High-fidelity hydrodynamic shape optimization of a 3-D hydrofoil. *J Ship Res* 2015;59(4):209–26. <http://dx.doi.org/10.5957/JOSR.59.4.150046>.
- [179] Liao Y, Martins JRRA, Young YL. 3-D High-fidelity hydrostructural optimization of cavitation-free composite lifting surfaces. *Compos Struct* 2021;268:113937. <http://dx.doi.org/10.1016/j.comstruct.2021.113937>.
- [180] Smith B, Brooks TR, Leader M, Chin TW, Kennedy GJ, Martins JRRA, Cesnik CES. Passive aeroelastic tailoring. Technical report CR-2020-220425, NASA; 2020.